

1 RESEARCH ARTICLE
2

3 **Opaque-2 Regulates a Complex Gene Network Associated with Cell**
4 **Differentiation and Storage Functions of Maize Endosperm**

5
6 Junpeng Zhan^{a,1,2}, Guosheng Li^{a,1}, Choong-Hwan Ryu^a, Chuang Ma^{a,3}, Shanshan Zhang^a, Alan
7 Lloyd^b, Brenda G. Hunter^a, Brian A. Larkins^{a,c}, Gary N. Drews^b, Xiangfeng Wang^{a,4}, and Ramin
8 Yadegari^{a,5}

9
10 ^a School of Plant Sciences, University of Arizona, Tucson, Arizona 85721

11 ^b Department of Biology, University of Utah, Salt Lake City, Utah 84112

12 ^c Department of Agronomy and Horticulture, University of Nebraska, Lincoln, NE 68588

13
14 ¹ These authors contributed equally to this work.

15
16 ² Current address: Donald Danforth Plant Science Center, St. Louis, Missouri 63132

17
18 ³ Current address: College of Life Sciences, Northwest A&F University, Yangling, Shaanxi 712100,
China.

19
20 ⁴ Current address: Department of Crop Genomics and Bioinformatics, China Agricultural University,
Beijing 100193, China.

21
22 ⁵ Address correspondence to yadegari@email.arizona.edu.

23 **Short Title:** Opaque-2 regulation of endosperm development

24
25 **One-sentence summary:** Genome-wide analysis of genes regulated by the maize transcription factor
26 Opaque-2 (O2) uncovered its functions in regulation of cell differentiation and endosperm storage
27 development.

28
29 The author responsible for distribution of materials integral to the findings presented in this article in
30 accordance with the policy described in the Instructions for Authors (www.plantcell.org) is: Ramin
31 Yadegari (yadegari@email.arizona.edu).

32
33
34 **ABSTRACT**

35 Development of the cereal endosperm involves cell differentiation processes that enable nutrient
36 uptake from the maternal plant, accumulation of storage products and their utilization during
37 germination. However, little is known about the regulatory mechanisms that link cell
38 differentiation processes with those controlling storage product synthesis and deposition,
39 including the activation of zein genes by the maize (*Zea mays*) bZIP transcription factor Opaque-
40 2 (O2). Here, we mapped *in vivo* binding sites of O2 in B73 endosperm, and compared the
41 results with genes differentially expressed in B73 and B73o2. We identified 186 putative direct
42 O2 targets and 1,677 indirect targets, encoding a broad set of gene functionalities. Examination
43 of the temporal expression patterns of O2 targets revealed at least two distinct modes of O2-

44 mediated gene activation. Two O2-activated genes, *bZIP17* and *NAKED ENDOSPERM2*
45 (*NKD2*), encode transcription factors, which can in turn co-activate other O2-network genes with
46 O2. *NKD2* (with its paralog *NKD1*) was previously shown to be involved in regulation of
47 aleurone development. Collectively, our results provide insights into the complexity of the O2-
48 regulated network and its role in regulation of endosperm cell differentiation and function.

49

50 INTRODUCTION

51 Endosperm is a filial seed structure that provides nutrients and signals essential for
52 embryogenesis and seedling germination (Li and Berger, 2012; Yan et al., 2014). In contrast to
53 dicotyledonous plants, such as *Arabidopsis thaliana*, in which the endosperm is eventually
54 absorbed in part by the developing embryo, the endosperm of cereals persists throughout seed
55 development, constitutes a large proportion of the mature grain, and accumulates large amounts
56 of storage compounds, including starch and storage proteins (Sabelli and Larkins, 2009; Li and
57 Berger, 2012). As such, cereal grains are a primary source of human calories and industrial raw
58 materials (FAO, 2015). Our understanding of how gene regulatory networks controlling storage
59 functions are activated during endosperm development, and their interplay with earlier
60 developmental process programs, such as cell differentiation, is limited.

61 Development of angiosperm seeds is initiated by double fertilization, during which one of two
62 sperm cells fuses with the egg cell to produce an embryo, and the other fertilizes the central cell
63 to produce the endosperm (Friedman et al., 2008; Hamamura et al., 2012). Upon fertilization in
64 maize (*Zea mays*) seed, the nucleus of the fertilized central cell (the primary endosperm cell)
65 undergoes free nuclear divisions, resulting in a coenocyte that becomes cellularized by
66 approximately 4 days after pollination (DAP) and then differentiates into four main cell types
67 that are distinguishable by about 6 DAP. These cell types are identified as the aleurone (AL),
68 basal endosperm transfer layer (BETL), embryo-surrounding region (ESR), and starchy
69 endosperm (SE). By about 8 DAP, further differentiation of the SE results in at least four distinct
70 subregions, namely the basal intermediate zone (BIZ), central starchy endosperm (CSE),
71 conducting zone (CZ), and subaleurone (SA). Concurrent with cell differentiation, mitotic
72 proliferation of the maize endosperm begins immediately after cellularization and lasts until
73 about 8 to 12 DAP in the CSE and 20 to 25 DAP in the SA and AL. Starting around 8 to 10 DAP,

74 the SE cells gradually switch from mitosis to endoreduplication, and begin accumulating storage
75 compounds. Maturation of SE cells begins about 16 DAP and involves programmed cell death
76 and desiccation (Becraft, 2001; Olsen, 2001, 2004; Sabelli and Larkins, 2009; Becraft and
77 Gutierrez-Marcos, 2012; Leroux et al., 2014; Zhan et al., 2017).

78 One of the key characteristics of highly differentiated SE cells is expression of storage-protein
79 genes (Sabelli and Larkins, 2009; Becraft and Gutierrez-Marcos, 2012). Prolamins, which
80 constitute the major storage proteins in maize endosperm, are termed zeins. Zeins are encoded by
81 distinct gene families and classified as α - (19- and 22-kD, including a total of 41 to 48 family
82 members), β - (15-kD, one family member), γ - (16-, 27-, and 50-kD, one family member each),
83 and δ -zein (10- and 18-kD, one family member each) (Coleman and Larkins, 1999; Woo et al.,
84 2001; Larkins et al., 2017). The bZIP family transcription factor (TF) Opaque-2 (O2) was shown
85 to regulate genes in nearly all these families through binding to a GENERAL CONTROL OF
86 NITROGEN4 (GCN4)-like motif (a.k.a. O2-box) (Schmidt et al., 1990; Schmidt et al., 1992;
87 Muth et al., 1996; Li et al., 2015). A mutation in *O2* results in opaque/starchy mature kernels that
88 have reduced levels of 22-kD α -zeins and increased lysine content (Mertz et al., 1964; Schmidt et
89 al., 1987). Previous transcriptome analyses of *o2* endosperm indicated that, in addition to
90 storage-protein gene expression, O2 regulates genes involved in a diverse array of biological
91 functions or processes, including synthesis and metabolism of carbohydrates and lipids (Hunter
92 et al., 2002; Jia et al., 2007; Frizzi et al., 2010; Hartings et al., 2011; Jia et al., 2013; Li et al.,
93 2015). Nonetheless, whether these processes are directly or indirectly regulated by O2 remains
94 largely unknown. Protein-DNA binding assays enabled identification of a number of direct target
95 genes of O2; the best characterized canonical targets of O2 include multiple zein genes of
96 various families, the *b-32* gene that encodes a 32-kD type I ribosome-inactivating protein
97 implicated in pathogen defense, the *cyPPDK1* gene that encodes an endosperm-specific cytosolic
98 isoform of pyruvate orthophosphate dikinase putatively involved in carbon partitioning, the
99 *Lysine-ketoglutarate reductase/Saccharopine dehydrogenase (LKR/SDH)* gene, which encodes a
100 bifunctional enzyme involved in lysine catabolism, and the *O2* gene itself (Lohmer et al., 1991;
101 Bass et al., 1992; Schmidt et al., 1992; Cord Neto et al., 1995; Gallusci et al., 1996; Maddaloni et
102 al., 1996; Kemper et al., 1999; Li et al., 2015).

103 Several observations suggest O2 functions in a complex with other regulatory proteins. First, O2
104 as a bZIP family protein can homodimerize or heterodimerize *in vitro* with the O2-
105 heterodimerizing proteins (OHPs)—OHP1 and OHP2—that are paralogs of O2 (Pysh et al., 1993;
106 Unger et al., 1993; Pysh and Schmidt, 1996; Xu and Messing, 2008). The OHPs are also capable
107 of binding *in vitro* the O2-box in zein gene promoters (Pysh et al., 1993; Yang et al., 2016).
108 Second, O2 has been shown to physically interact with the DOF family TF Prolamin-box binding
109 factor (PBF) *in vitro* (Vicente-Carbajosa et al., 1997). Third, PBF and OHP1/OHP2 have been
110 shown to interact *in vitro* and *in vivo* (Zhang et al., 2015). Genetic analyses have shown that O2,
111 the OHPs, and PBF co-activate expression of zein genes in a synergistic or additive manner, with
112 O2 playing the major role in regulation of 19- and 22-kD α -zein genes and the OHPs playing the
113 major role in regulation of the 27-kD γ -zein gene (Zhang et al., 2015; Yang et al., 2016). In
114 addition, O2 has also been shown to interact with several other nuclear proteins, including the
115 MADS-box family TF protein MADS47, the transcriptional-adaptor protein
116 Alteration/deficiency in activation2 (ADA2) and the histone acetyltransferase General control of
117 nitrogen5 (GCN5) to co-regulate O2 target gene expression (Bhat et al., 2003; Bhat et al., 2004;
118 Qiao et al., 2016). The partnership of O2 with multiple nuclear factors is likely associated with
119 the complexity of the O2 gene regulatory network (GRN).

120 Here, we used RNA sequencing (RNA-Seq) and chromatin immunoprecipitation followed by
121 high-throughput sequencing (ChIP-Seq) to identify genes directly or indirectly regulated by O2
122 in maize endosperm. By RNA-Seq, we identified 1,863 genes differentially expressed between
123 the wild-type B73 (WT) and B73o2. Among these, 186 genes were detected by ChIP-Seq as
124 putative direct targets of O2. Analyses of the direct and indirect O2 targets revealed a broad role
125 for O2 in the regulation of the gene expression programs associated with multiple key aspects of
126 endosperm development and function. An analysis of the temporal expression patterns of O2
127 targets in WT versus mutant endosperm indicated two distinct modes of gene activation. The
128 observation that O2 directly activates two genes encoding TF proteins, which in turn co-regulate
129 direct target genes with O2, provides novel insight into the key players of the O2 GRN and a
130 potentially important role for O2 in aleurone cell differentiation.

131

132 RESULTS

133 **Identification of O2 target genes using chromatin immunoprecipitation coupled with
134 differential expression analysis**

135 To identify O2-regulated genes, we first screened for genes differentially expressed in the
136 endosperm of B73 versus B73 α 2 (the genetic confirmation of the B73 α 2 mutant is described in
137 the Methods and Supplemental Figure 1) using RNA-Seq of 15-DAP endosperm, a stage shortly
138 after the initiation of the storage program (Sabelli and Larkins, 2009; Li et al., 2014). For each
139 genotype, total RNAs extracted from biological triplicates were polyA-selected, reverse-
140 transcribed to cDNA, and sequenced using an Illumina HiSeq 2500 platform. Between
141 52.9 and 66.8 million paired-end reads were obtained for each sample; 92.3% to 93.3% of the
142 reads were mapped to the maize reference genome. After excluding genes expressed at extremely
143 low levels, the remaining 28,580 genes were normalized by edgeR, and statistically tested for
144 differential expression. Among the tested genes, 1,863 were detected as differentially expressed
145 genes (DEGs) [false discovery rate (FDR) < 0.05], including 1,024 that were downregulated
146 [\log_2 -transformed fold change (FC) < 0] and 839 upregulated (\log_2 FC > 0) in the α 2 mutant
147 (Figure 1A).

148 We evaluated the quality of our RNA-Seq data in two ways. First, we used pairwise Spearman
149 correlation coefficient (SCC) analysis of the normalized reads (in RPKM) of all the genes tested
150 for differential expression. This analysis revealed SCCs ranging from 0.92 (biological replicates
151 2 versus 3) to 0.95 (biological replicates 1 versus 2, and 1 versus 3) for the WT samples and 0.96
152 (biological replicates 1 versus 3, and 2 versus 3) to 0.97 (biological replicates 1 versus 2) for the
153 B73 α 2 samples that indicated high reproducibility of the sampling. Second, we compared our
154 data to the previously published reports of the O2-modulated genes. An examination of
155 expression levels of several canonical direct O2 targets showed that almost all the known targets,
156 as exemplified by O2 itself, a 22-kD α -zein gene (*azs22-4*) and the *LKR/SDH* gene, were
157 dramatically downregulated in our mutant data (Supplemental Data Set 1). We also compared
158 our DEGs with the DEGs identified by prior transcriptomic studies of α 2 mutants by mapping
159 the published transcript/probe sequences [available for four reports (Hunter et al., 2002; Frizzi et
160 al., 2010; Jia et al., 2013; Zhang et al., 2016)] to the B73 cDNAs using the BLAT program (Kent,
161 2002). The result showed the DEGs that we identified included 494 genes that have been
162 detected by at least one prior study (Supplemental Figure 2A). Surprisingly, among these 494

163 genes, only 6 have been commonly identified by all four previous studies (Supplemental Figure
164 2A). An analysis of the expression level of DEGs detected by previous studies but not by us
165 showed that nearly all of them exhibited low fold-changes ($|\log_2\text{FC}| < 1$) in our dataset
166 (Supplemental Figure 2B).

167 To determine the genome-wide direct target genes of O2, we performed a ChIP-Seq assay on two
168 biological replicates of B73 endosperm at 15 DAP using a previously described anti-O2 antibody
169 (Schmidt et al., 1992). As a negative control, we performed the same assay in duplicates using
170 endosperm from B73o2. The recovered genomic fragments were sequenced using an Illumina
171 HiSequation 2500 platform to generate paired-end reads. Each sample produced 25.6 to 38.3
172 million reads of which 68.4% to 79.8% were mapped to the maize reference genome. Mapped
173 reads of the biological replicates for each genotype were subsequently merged and used to
174 identify O2-bound sequences using MACS software (Zhang et al., 2008; Feng et al., 2012). With
175 a cutoff *q*-value of 0.05, MACS detected 6,365 peaks corresponding to putative O2-bound
176 regions in the maize genome. A major fraction (70.0%) of the identified peaks were located >5
177 kb away from the gene models (Figure 1B) as previously described for other maize TFs
178 (Morohashi et al., 2012; Eveland et al., 2014). However, this was a higher fraction than
179 previously reported by Li et al. (2015), who showed that 66% of the O2 peaks were located
180 within 1 kb up- or downstream of gene models. We defined O2-bound genes as those with peaks
181 detected in the genic regions or within 5 kb up- or downstream of the annotated gene models.
182 Based on these criteria, 3,282 putative O2-bound genes were identified (Supplemental Data Set
183 2). Of the peaks associated with these genes, most were located within either 5 kb upstream (18.5%
184 of all peaks) or 5 kb downstream (8.5%) to the gene models, while much smaller fractions were
185 located within intronic (2.7%), 5'-untranslated region (UTR; 0.1%), coding DNA sequence
186 (CDS; 0.1%), or 3'-UTR (0.1%) sequences (Figure 1B).

187 Overlay of the identified O2-bound genes with the O2-modulated genes identified 186 bound
188 modulated genes (here referred to as direct target genes of O2), including 147 shown to be O2
189 activated and 39 as O2 repressed (Figure 1C; Supplemental Data Set 3). By exclusion, the
190 unbound modulated genes (here referred to as the indirect targets of O2, which are likely to
191 include genes whose transcription is regulated by TFs downstream to O2) included 877 O2-

192 activated genes and 800 O2-repressed genes, while the group that was detected as bound but
193 unmodulated by O2 included 3,096 genes (Figure 1C).

194 To evaluate the accuracy of our identification of direct O2 targets, we examined the differential
195 expression and peak association of several canonical O2 targets including *O2* itself, *cyPPDK1*,
196 *azs22-4*, *LKR/SDH*, *b-32*, and the 15-kD β -zein gene (Lohmer et al., 1991; Schmidt et al., 1992;
197 Cord Neto et al., 1995; Gallusci et al., 1996; Maddaloni et al., 1996; Kemper et al., 1999). The
198 results showed that nearly all of these genes are identified as direct O2 targets by our data
199 (Supplemental Figure 3 and Supplemental Data Set 3). The only exception was the *b-32* gene,
200 which exhibited a dramatic downregulated pattern in the B73*o2* mutant ($\log_2\text{FC} = -9.65$;
201 Supplemental Data Set 1) but was not associated with an O2 peak. By applying a similar cutoff
202 criterion as used by Li et al. (2015) to define O2-bound genes, which is that an O2-bound gene is
203 defined as a gene with one or more O2 peak(s) detected in the genic regions or within 1 kb up- or
204 downstream of the annotated gene models, we detected 1,057 O2-bound genes [versus 1,143
205 detected by Li et al. (2015)], including 98 putative O2-activated [versus 35 detected by Li et al.
206 (2015)] and 17 putative O2-repressed [versus 4 detected by Li et al. (2015)] direct target genes
207 (Supplemental Figure 4A). Comparison of the 98 O2-activated direct target genes versus the 35
208 O2-activated direct targets identified by Li et al. (2015) produced only 13 genes in common
209 between the two studies (Supplemental Figure 4B).

210 To gain insight into the association of O2-modulated and/or bound gene sets with O2-binding
211 sites, we summarized the previously reported O2-binding sequences from the literature
212 (Supplemental Table 1) and determined the occurrences of these sequences within the 5'-
213 regulatory regions of O2-modulated and/or bound gene sets. The result showed a relatively larger
214 fraction of the direct targets was associated with known O2-binding sites as compared to the
215 indirect targets or the bound unmodulated genes (Supplemental Figure 5). Correspondingly, the
216 enrichments of the O2-binding-site-associated genes among the activated direct targets and the
217 bound unmodulated genes were statistically significant ($P < 10^{-5}$, hypergeometric test),
218 suggesting that our ChIP-Seq analysis successfully distinguished direct O2 targets from indirect
219 targets with respect to the association with previously identified O2-binding sites. Notably, only
220 a small fraction of O2-bound genes (630/3,282) were associated with previously identified O2-

221 binding sites, suggesting that O2 likely binds additional *cis*-regulatory sequences that are yet to
222 be characterized (see below).

223 We next evaluated the extent to which the absence of O2 modified the endosperm transcriptome
224 either directly or indirectly through a boxplot analysis of the log₂-transformed reads per kilobase
225 per million mapped reads (RPKM) data. This analysis indicated the O2-activated direct targets
226 showed the largest decrease in overall gene expression in the mutant, as compared to WT
227 endosperm (average log₂FC = -3.75) (Figure 1D). Conversely, the O2-activated indirect targets
228 and the O2-repressed genes (both direct and indirect) showed a more modest mRNA level
229 increase in the mutant (average log₂FC = -1.92, 1.98, and 1.90, respectively). These data suggest
230 that the O2-activated, direct target gene set is most crucially dependent on regulation by O2
231 compared to the other O2-modulated and/or bound gene sets.

232 An analysis of the expression patterns of the O2-activated direct targets using the available maize
233 gene expression atlas (Chen et al., 2014a) showed that expression of these genes is highly
234 endosperm specific, mirroring the pattern of *O2* itself (Supplemental Figure 6). Interestingly, the
235 expression of the O2-repressed direct targets also showed slightly higher expression in the
236 endosperm/kernel than in other tissues. However, their median expression levels were
237 consistently lower than the O2-activated direct targets throughout endosperm/kernel
238 development, and the differences were extremely significant ($P < 0.001$, Student's *t* test) for all
239 the examined developmental stages after 8 DAP (Supplemental Figure 6).

240 Based on our criteria for defining O2-bound genes, we detected 166 O2 peaks within the range
241 of -5 kb to +5 kb of the gene models of the 186 direct O2 target genes (Supplemental Data Set 3).
242 To gain insights into the O2-binding sites among these genes, we profiled their distribution by
243 counting the number of peaks per 100-bp bins and found an enrichment within the -400 to +100
244 bp genomic regions (Figure 1E). Profiling the read distribution over the same annotated gene
245 models using a similar approach confirmed this pattern (Supplemental Figure 7). These results
246 were consistent with the reported localization of several known O2-binding sites, which were
247 detected within the 300-bp region upstream of the translation start sites (Schmidt et al., 1992;
248 Wu and Messing, 2012). We used two independent approaches to verify binding of O2 to the O2
249 peaks. First, using electrophoretic mobility shift assays (EMSA), we tested 9 peaks (or 5'-
250 regulatory regions that partially overlap with an O2 peak) associated with O2-activated genes,

251 including the 18-kD δ -zein gene, *bZIP17*, *G-box binding factor1 (GBF1)*, *bZIP104*,
252 *GRMZM2G084296*, *NAC78*, *NAKED ENDOSPERM2 (NKD2)*, and *Tryptophan
aminotransferase-related3 (TAR3)*, and one peak that was associated with the O2-repressed gene
253 *GRMZM2G443668* (Supplemental Table 2). The results showed that all the tested sequences
254 were bound by O2, and that the binding activity could be partially or completely abolished by
255 addition of competitor probes containing O2-binding sequences (Supplemental Figure 8). Second,
256 in dual luciferase reporter (DLR) assays performed in *Nicotiana benthamiana* with the O2
257 protein fused with a strong transcription activation domain (Supplemental Figure 9A), seven out
258 of 13 peaks were confirmed to be bound by O2 ($P < 0.05$, Student's *t* test) (Supplemental Figure
259 9B and Supplemental Table 3). Among these seven, six were associated with O2-activated genes,
260 including the 15-kD β -zein gene, the 18-kD δ -zein gene, *Floury-2 (FL2)*, *bZIP17*, *NKD2*, and
261 *TAR3*; one was associated with an O2-repressed gene, *LIP15* (encoding a 15-kD low
262 temperature-induced protein).

264 To identify additional *cis*-regulatory sequences that mediate O2 binding and gain further insight
265 into the protein complex involved in regulation of O2 target genes, we performed an analysis of
266 DNA sequence motifs enriched within a 401-bp region centered at the summits of each of the
267 166 peaks for the direct O2 target genes using MEME-ChIP software (Machanick and Bailey,
268 2011). This analysis identified 19 motifs (*E*-value < 0.05 ; Supplemental Table 4), two of which
269 (Motifs 5 and 15) contained a common sequence CCACGTCA that is very similar to several
270 known plant bZIP motifs characterized by an ACGT core sequence ($P < 0.05$). Both motifs were
271 shown to be centrally enriched in the analyzed genomic regions ($P < 0.05$) (Figure 1F;
272 Supplemental Table 4). These results indicate that Motifs 5 and 15 likely contain the *cis*-
273 regulatory sequences bound by O2.

274 In addition, MEME-ChIP also identified several significantly enriched *cis*-motifs that were not
275 centrally enriched (Supplemental Table 4). The presence of these motifs within the detected O2-
276 bound genomic regions suggests that they could contain binding sites of other TFs that co-
277 regulate target genes in collaboration with O2. For example, the most prevalent sequence
278 variants of Motif 2 all contain TGTAAG (Supplemental Table 4), which is indeed identical to
279 the core sequence of the known PBF-binding site (*i.e.*, the P-box) (Vicente-Carbajosa et al.,
280 1997). Consistent with previous reports showing the co-existence of the O2-box and P-box in the

281 promoter regions of seed storage-protein genes (Vicente-Carbajosa et al., 1997; Hwang et al.,
282 2004), the enrichment of Motif 2 suggests that many of the direct O2 targets are co-regulated by
283 PBF or, alternatively, other endosperm-expressed DOF family TFs. These results support the
284 notion that many additional TFs, including the canonical O2-interacting TF PBF, are involved in
285 the regulation of O2 target genes in combination with O2.

286

287 **O2 regulates a diverse set of genes involved in endosperm storage product synthesis and**
288 **accumulation**

289 To gain a comprehensive understanding of the functions of the O2-regulated gene network, we
290 identified the GO terms significantly enriched ($FDR < 0.05$) among the O2 target genes (directly
291 activated/repressed and indirectly activated/repressed) using Blast2GO software (Gotz et al.,
292 2008). The most significantly enriched GO term for the O2-activated direct targets is “nutrient
293 reservoir activity” (Figure 2A), with nearly all the associated genes encoding zein proteins (21 of
294 22, with GRMZM2G325920 annotated as having an uncharacterized function). A less significant
295 molecular function enriched for these genes is “proline dehydrogenase activity,” which is
296 associated with two proline oxidase genes (GRMZM2G053720 and GRMZM2G117956). The
297 most significant biological process enriched for this target gene set is “carboxylic acid metabolic
298 process,” which is associated with 16 genes, including the *LKR/SDH*, *cyPPDK1*, and *cyPPDK2*
299 genes, while the other two associated enriched biological processes are “glutamine family amino
300 acid biosynthetic process” and “proline catabolic process”. Consistent with the GO term
301 enrichments, an analysis of metabolic pathways associated with the O2-activated direct targets
302 using the CornCyc tool revealed genes involved in glycine biosynthesis, L-glutamine
303 biosynthesis, proline metabolism (as part of the L-N^δ-acetylornithine biosynthesis pathway) and
304 L-glutamate degradation (Supplemental Data Set 4). Together, these GO term enrichments and
305 pathway associations indicate that O2 directly activates genes encoding storage proteins and
306 enzymes involved in amino acid synthesis and metabolism, and regulates genes associated with
307 partitioning of carbon between carbohydrates and proteins in maize endosperm.

308 We also closely examined all the known zein genes as canonical direct targets of O2 for
309 expression and O2 binding. Of the 40 zein genes annotated in the B73 genome (Chen et al.,
310 2014a), three genes, including one 22-kD α -zein (GRMZM2G535393) and two 19-kD z1A sub-

family α -zein genes (GRMZM2G489581 and GRMZM2G514379), were excluded from our differential gene expression analysis due to low levels of expression; of the remaining 37 zein genes, 34 were shown to be modulated by O2 and three (all γ -zein genes) did not display significant differential expression levels at 15 DAP, although they were found to be bound by O2 (Figure 3). All the differentially expressed zein genes were downregulated in the *o2* mutant ($\log_2\text{FC} < -4.0$), indicating that O2 is an activator of all the modulated zein genes. The combination of the differential gene expression analysis and O2-binding data suggested that different zein families are regulated by O2 in different manners at 15 DAP. The 15-kD β -zein and the 18-kD δ -zein genes are directly activated by O2, whereas the α -zein gene family members (31 genes) were identified as either direct or indirect target genes of O2 (Figure 3). Among the latter, the 19-kD α -zein gene sub-families, z1A and z1B, and the 22-kD α -zein gene family each included both direct and indirect target genes, while the 19-kD subfamily, z1D, included only indirect targets (Figure 3). Furthermore, different families of zein genes were shown to be downregulated in the mutant to different extents. The most dramatically downregulated gene family was the 22-kD α -zein family, with $\log_2\text{FC}$ ranging from -10.5 to -9.8, while the 19-kD α -zein sub-families, z1A, z1B, and z1D, showed a relatively lower extent of downregulation, with $\log_2\text{FC}$ ranging from -8.7 to -7.6, -7.5 to -5.3, and -9.36 to -4.79, respectively (Figure 3 and Supplemental Data Set 1). These data suggest the 22-kD α -zein family is most crucially dependent on activation by O2, consistent with a previous report showing that the 22-kD zein proteins are almost absent in *o2* endosperm, while other zein proteins are reduced to a lesser extent (Kodrzycki et al., 1989). As noted above, the γ -zein genes (including the 16-kD, 27-kD, and 50-kD zeins) are associated with O2 peaks, but are not modulated by O2 based on our data (Figure 3); this observation suggests that although O2 binds upstream regions of some target genes, their expression is not significantly dependent on this binding, at least at the assayed stage of 15 DAP.

The O2-activated indirect targets are enriched for a more diverse set of GO terms, likely due to the larger number of associated genes as compared to the direct targets (Figure 2B). Notably, the most significantly enriched GO term for this gene set is also “nutrient reservoir activity,” which is associated with 16 genes, including at least 10 known zein genes (see above). Accordingly, many other GO terms enriched for this gene set, including the molecular functions “3-deoxy-7-phosphoheptulonate synthase activity,” “2-oxoisovalerate dehydrogenase (acylating) activity,”

342 and “methylmalonate-semialdehyde dehydrogenase (acylating) activity,” and the biological
343 processes “aromatic amino acid family biosynthetic process,” and “valine biosynthetic process,”
344 are associated with amino acid or protein synthesis/metabolism. Likewise, metabolic pathway
345 analysis also detected genes involved in synthesis of aromatic compounds (*e.g.*, chorismate, 4-
346 hydroxybenzoate, and benzoate) or branched-chain amino acids among the indirect target genes
347 (Supplemental Data Set 4).

348 Interestingly, the O₂-activated indirect targets are also enriched for many GO terms related to the
349 synthesis/metabolism of carbohydrates and lipids. For example, the most significantly enriched
350 biological process, “single-organism carbohydrate metabolic process,” is associated with 41
351 genes, including the genes encoding a sucrose synthase [*Sucrose synthase2 (SUS2)*], a malate
352 synthase [*Malate synthase1 (MAS1)*], a glucose-1-phosphate adenyltransferase [*ADP glucose*
353 *pyrophosphorylase2 (AGP2)*], and two fructokinases [*Fructokinase1 (FRK1)* and *FRK2*]
354 involved in carbohydrate synthesis/degradation pathways (Supplemental Data Set 4). On the
355 other hand, this gene set is enriched for many lipid storage/metabolism-associated GO terms,
356 including “acyl-CoA oxidase activity,” “lipid metabolic process,” “lipid storage,” and
357 “monolayer-surrounded lipid storage body,” and the metabolic pathway analysis confirmed the
358 putative functions of many of these genes in the biosynthesis/metabolism of lipid/fatty acids
359 (Supplemental Data Set 4). In addition, the O₂-activated indirect targets are also enriched for
360 “response to abiotic stimulus,” “response to herbicide,” “response to absence of light,” “response
361 to desiccation,” etc., suggesting that O₂ also indirectly regulates abiotic stress responses of the
362 endosperm.

363 The subset of genes identified as directly repressed by O₂ did not show significant enrichment of
364 any GO terms, which was likely due to the limited functional annotations for most of these genes.
365 The genes with available annotation included only three TF genes (*LIP15*, *MYBR10*, and
366 *Orphan154*) and one diacylglycerol O-acyltransferase gene (GRMZM2G042356) that functions
367 in triacylglycerol biosynthesis (Supplemental Data Set 3). Manual inspection of putative
368 functions of the other genes in this group identified a putative sugar transporter gene
369 (GRMZM2G159559) and a putative glutathione γ -glutamylcysteinyltransferase gene
370 (GRMZM2G038170) (Supplemental Data Sets 5 and 6) that are likely associated with storage
371 product synthesis/metabolism. On the other hand, the gene subset identified as O₂-repressed

372 indirect targets is most significantly enriched for the biological process “translational termination”
373 and the molecular function “translation release factor activity, codon specific” (Figure 2C),
374 indicating that O2 likely facilitates storage product synthesis and deposition in the endosperm
375 through indirect repression of translational termination. In addition, this group of genes is also
376 enriched for “protein serine/threonine kinase activity” and “protein phosphorylation,” suggesting
377 O2 indirectly represses a protein kinase activity in the endosperm. Taken together, O2 directly or
378 indirectly regulates a large number of downstream genes involved in the synthesis/metabolism of
379 a wide range of storage products deposited in the endosperm, including storage proteins,
380 carbohydrates, and lipids.

381

382 **Two modes of O2-mediated gene activation can be distinguished from the temporal
383 patterns of target gene expression**

384 To understand the dynamics of O2 network gene expression during early endosperm
385 development, we interrogated the previously identified time-course programs of endosperm
386 mRNA accumulation (Li et al., 2014) for timing of *O2* activation versus its targets. Based on the
387 temporal expression data, *O2* exhibits an “up@8DAP” pattern; that is, it showed relatively low
388 expression in 0- through 6-DAP kernels, but high expression in 8-, 10-, and 12-DAP endosperm.
389 Comparison of the O2-modulated and/or bound gene sets with the temporally upregulated gene
390 sets showed the O2-activated direct targets significantly overlap with the up@8DAP and
391 up@10DAP gene sets ($P < 10^{-5}$, hypergeometric test) (Figure 4A). Similarly, the O2-activated
392 indirect target gene set also significantly overlaps with up@8DAP and up@10DAP gene sets
393 (Figure 4A), indicating similar activation timing of both the direct and indirect targets of O2.
394 Interestingly, a significant portion of the O2-repressed indirect target gene set also shows an
395 upregulated pattern at 8 and 10 DAP in WT endosperm (*i.e.*, up@8DAP and up@10DAP)
396 (Figure 4A). This suggests a role for O2 in dampening or tightly modulating the expression of
397 genes activated through O2-dependent or O2-independent activation during early endosperm
398 development. These results nonetheless suggest the temporal upregulation of a substantial
399 portion of the direct and indirect O2 targets correlates strongly with O2’s upregulation.

400 From our previous temporal data, we also detected a significant number of O2-activated indirect
401 target genes that show a temporally upregulated pattern in the WT kernel/endosperm at 4 or 6

402 DAP (*i.e.*, up@4DAP or up@6DAP) (Figure 4A), preceding the detected upregulation of *O2* at 8
403 DAP (Li et al., 2014). Coincidentally, we also detected a handful of direct targets as showing the
404 same upregulated pattern at 4 and 6 DAP (Figure 4A). Therefore, we hypothesize that a portion
405 of the *O2*-regulated network is activated by an *O2*-independent process and then subsequently
406 maintained or further activated by *O2* after 8 DAP. To test this, we used reverse transcription
407 quantitative PCR (RT-qPCR) to measure the mRNA levels of representative genes that were
408 detected to be directly or indirectly activated by *O2*, including *O2* itself, in a developmental time
409 series of B73 and B73 o2 endosperm from 6 to 30 DAP (Figures 4B to 4M; Supplemental Data
410 Set 8). Among the 18 *O2*-activated direct targets tested, 11 genes were significantly
411 downregulated in the *o2* mutant at 12, 15, and/or 18 DAP (Figures 4C to 4M; Supplemental Data
412 Set 8). Surprisingly, these genes exhibited at least two distinct temporal patterns of activation in
413 the WT. Group 1 genes showed either an undetectable [*b-32* and GRMZM2G025763 (a 19-kD
414 z1B sub-family α -zein gene)] or nearly undetectable (*azs22-4* and the 15-kD β -zein gene) level
415 of expression in the WT before *O2* mRNA was detected (6 to 8 DAP; Figure 4B), and showed
416 increased expression at subsequent stages (Figures 4C to 4F). On the other hand, Group 2 genes,
417 including the 18-kD δ -zein gene, *bZIP17*, *GBF1*, GRMZM2G117956, *LKR/SDH*, *NAC122*, and
418 *NKD2*, are already highly expressed, even before the detectable accumulation of *O2* mRNA [Ct
419 $\leq 31.37 \pm 2.31$ (mean \pm SEM) at 6 DAP] (Figures 4G to 4M). These results suggest *O2* is
420 required for the early activation of Group 1 genes, whereas activation of Group 2 genes is *O2*
421 independent. In addition, for all Group 2 genes, the most dramatic downregulation in mutant
422 endosperm was observed at 15 or 18 DAP, indicating *O2* is essential for maintenance of their
423 expression. Therefore, not all *O2* direct target genes are necessarily activated by *O2* during early
424 stages (6 to 8 DAP) of endosperm development, some being activated via *O2*-independent
425 regulatory processes. Moreover, it is noteworthy that all genes in Groups 1 and 2, as well as *O2*
426 itself, exhibit a dramatic temporal upregulation during 15 or 18 DAP to 22 DAP in the *o2*
427 background, with some genes showing mRNA levels as high as those of WT by 22 DAP
428 (Figures 4B to 4M). These results highlight a late, *O2*-independent gene regulatory program that
429 is also responsible for maintaining a high expression level of the *O2*-activated direct targets later
430 in endosperm development. Taken together, *O2* regulates a highly dynamic network of genes
431 whose regulation punctuates three periods of endosperm development.

432

433 **O2 directly activates a novel O2-heterodimerizing-protein gene**

434 To identify key regulatory components of the O2 network, we explored the nature of TF genes
435 acting downstream of O2. Our RNA-Seq analysis detected at least 93 TF genes modulated by O2
436 (Supplemental Data Set 1). Overlay of the O2-modulated genes with the O2-bound genes
437 identified 15 of the 93 TF genes as putative direct O2 target genes, including 12 O2-activated
438 and three O2-repressed TF genes; the former included 4 bZIP genes (including *O2* itself), 3 NAC
439 genes, 2 Homeobox genes, and 3 genes belonging to the C2H2, C3H, and CCAAT-HAP5
440 families, respectively, while the latter included a bZIP gene, a MYB-related gene, and a putative
441 TF gene without a recognized gene family (*Orphan154*) (Supplemental Data Set 3). An analysis
442 of the expression patterns of these O2-regulated TF genes throughout development showed that,
443 similar to *O2*, most of these genes are preferentially expressed in the endosperm, albeit at
444 relatively lower levels than *O2* (Figure 5). Notably, two of the five bZIP genes, namely *LIP15*
445 (repressed by O2) and *GBF1* (activated by O2), have been shown to be induced by low
446 temperature and hypoxia, respectively (de Vetten and Ferl, 1995; Kusano et al., 1995). The
447 recently characterized C2H2 zinc finger gene, *NKD2*, encoding one of the two paralogous
448 INDETERMINATE domain TFs (*NKD1* and *NKD2*) that are central regulators of many
449 endosperm developmental processes, including proper aleurone and starchy endosperm cell
450 differentiation and storage product deposition (Yi et al., 2015; Gontarek et al., 2016), was also
451 detected as an O2-activated direct target gene (Supplemental Data Set 3). Together, the detection
452 of these 15 TF genes as direct targets of O2 suggests a broad, direct role for O2 in endosperm
453 development that encompasses regulation of cell differentiation, storage function, and responses
454 to abiotic stresses.

455 Nearly 78 TF genes corresponding to 29 different TF families were detected among indirect O2
456 target genes (58 O2-activated and 20 O2-repressed genes). Many of these were shown to be
457 involved in regulation of various aspects of endosperm development. For instance, the O2-
458 repressed genes included *PBF*, is another key regulator of the endosperm storage program
459 discussed above. *PBF* mRNA is increased by about two-fold in B73o2 ($\log_2\text{FC} = 0.98$;
460 Supplemental Data Set 1), suggesting *PBF* expression is indirectly repressed by O2 in WT. In
461 addition, among the O2-activated indirect targets is the recently reported *Floury-3* gene, which
462 encodes a PLATZ family TF that functions in grain filling (Li et al., 2017), and the *Viviparous-1*

463 (*VPI*) gene, which encodes an ABI3-VP1 family TF that plays an essential role in regulation of
464 maize seed maturation and germination (Hoecker et al., 1995). Therefore, as each O2-regulated
465 TF likely regulates a set of target genes in the endosperm, the direct or indirect regulation of the
466 TF genes by O2 can in part explain the large number (1,677) of indirect O2 targets and their
467 associated diversity of biological functions.

468 To further understand the nature of TF genes under O2 regulation, we tested for enrichment of
469 the annotated TF gene families among the O2-modulated and/or bound gene sets and detected a
470 significant enrichment of bZIP family TF genes among the O2-activated direct targets ($P =$
471 3.1×10^{-5} , hypergeometric test) (Supplemental Figure 10). To understand the relatedness between
472 O2 and the (other) O2-regulated bZIP genes, we performed a phylogenetic analysis of all the
473 annotated maize bZIP proteins. This phylogeny shows that the proteins encoded by two of the
474 O2-regulated bZIP genes—*bZIP17* and *bZIP104*—are in fact in the same well-supported clade as
475 O2 and the previously reported OHP proteins (Supplemental Figure 11). Therefore, we
476 hypothesized that *bZIP17* can form a heterodimer with O2 and co-regulate O2 target genes with
477 it, and we tested this hypothesis using three approaches. First, we performed a reciprocal set of *in*
478 *vitro* pull-down assays of HA-/Myc-tagged O2 with Myc-/HA-tagged *bZIP17* proteins; these
479 showed the two proteins interact *in vitro* (Supplemental Figure 12). Second, we tested the O2-
480 *bZIP17* interaction *in vivo* using bimolecular fluorescence complementation (BiFC) assay in leaf
481 epidermal cells of *N. benthamiana*. O2 and *bZIP17* were fused to the N- and C-terminal portions,
482 respectively, of a yellow fluorescent protein (YFP) variant, Venus; in this assay, strong
483 fluorescence was observed in nuclei of *N. benthamiana* leaf cells infiltrated with O2-Venus^N plus
484 *bZIP17*-Venus^C but not in controls (Figure 6A). Third, to understand if O2 and *bZIP17* can co-
485 activate target gene expression, we tested the six peaks associated with O2-activated targets and
486 confirmed to be bound by O2 in *N. benthamiana* (Supplemental Figure 9B) for gene co-
487 activation by O2 and *bZIP17* using the DLR assay with the TFs each expressed as an intact
488 protein (Supplemental Figure 13). For one of the six peaks that was upstream of the *FL2* gene
489 (encoding a 22-kD α -zein protein), reporter gene expression was significantly elevated when O2
490 and *bZIP17* were both expressed compared to when O2 alone was expressed [$P < 0.05$, one-way
491 ANOVA with post-hoc Tukey's honestly significant difference (HSD) test] (Figure 6B;
492 Supplemental Table 5). This indicates *bZIP17* can enhance O2-mediated *trans*-activation of *FL2*
493 by binding to the associated O2 peak, whereas *bZIP17* alone was unable to *trans*-activate it.

494 Together, these data suggest O2 interacts with bZIP17, and they can co-activate at least a subset
495 of target genes in a synergistic manner, likely through binding to the same *cis*-regulatory
496 sequence in the form of a bZIP heterodimer.

497

498 **O2 and NKD2 co-regulate a gene network associated with aleurone cell differentiation**

499 Our identification of *NKD2* as a direct target of O2 suggested that O2 and NKD2 co-regulate a
500 downstream gene network with direct mutual regulation. The NKD TFs have previously been
501 shown to directly *trans*-activate expression of *O2* and a 22-kD α -zein gene in isolated aleurone
502 protoplasts (Gontarek et al., 2016). A reported transcriptome analysis of a *nkd1;2* double mutant
503 coupled with analysis of NKD2-binding sites led to identification of 1,059 and 1,050 putative
504 direct targets of NKD2 in the starchy endosperm and aleurone, respectively (Gontarek et al.,
505 2016). We identified a total of 34 of these genes as direct O2 targets in our analysis, and the
506 overlap was significant ($P = 1.7 \times 10^{-26}$, hypergeometric test) (Figure 7A; Supplemental Table 6).
507 To understand if NKD2 and O2 can co-regulate target gene expression through O2-bound
508 sequences, we performed DLR assays on the six peaks associated with O2-activated targets and
509 confirmed to be bound by O2 in *N. benthamiana* (Supplemental Figure 9B), with O2 and NKD2
510 each expressed as intact proteins (Supplemental Figure 13 and Supplemental Table 7). In fact,
511 five of these peaks were determined to be associated with putative common direct targets of O2
512 and NKD2, including the 15-kD β -zein gene, the 18-kD δ -zein gene, *FL2*, *TAR3*, and *NKD2*
513 itself (Supplemental Table 3). The results showed that O2 and NKD2 co-activate three of the six
514 peaks in a synergistic manner (Figure 7B), suggesting the two TFs act collaboratively to activate
515 a portion of the O2- and NKD2-regulated gene networks. As a TF that functions immediately
516 downstream of O2, we hypothesized that NKD2 could directly regulate a subset of the indirect
517 O2 target genes. To test this hypothesis, we examined the indirect O2 target genes for the
518 presence of putative NKD2 direct target genes (Gontarek et al., 2016). The result showed that
519 120 of the 1,677 indirect O2 gene targets are likely regulated directly by NKD2 in starchy
520 endosperm and/or aleurone based on a significant overlap ($P = 1.3 \times 10^{-44}$, hypergeometric test)
521 (Figure 7C; Supplemental Data Set 7). These results indicate that NKD2 can act both as a co-
522 activator and as a downstream effector of O2 in regulation of both its direct and indirect target
523 genes.

524 The above data suggest that O2 could perform a role in aleurone development by regulating
525 NKD2 and its downstream genes. In support of this notion, examination of *O2* mRNA levels in
526 8-DAP maize kernel compartments [using laser-capture-microdissection (LCM)-derived
527 transcriptome data (Zhan et al., 2015)] revealed a relatively high expression level of *O2* in the
528 aleurone [fragments per kilobase of transcript per million mapped reads (FPKM) = 8.58], with a
529 ranking only second to the central starchy endosperm (FPKM = 71.65) (Figure 7D). Moreover,
530 an analysis of the overlapping genes between the gene sets specifically expressed in each of the
531 endosperm compartments (cell types) identified in the same study and the O2-modulated and/or
532 bound gene sets identified here showed both O2 activated direct and indirect target gene sets
533 overlap most significantly ($P = 1.8 \times 10^{-6}$ and 4.1×10^{-37} , respectively) with the aleurone-specific
534 gene set, compared to the other cell-type-specific gene sets (Figure 7E). Together, these data
535 suggest a strong association between expression of the O2 network genes and aleurone
536 differentiation.

537

538 DISCUSSION

539 We began dissecting the O2 GRN in maize endosperm by identifying endosperm-expressed
540 genes directly or indirectly regulated by O2. The mRNA profiling of 15-DAP endosperm from
541 B73 $o2$ versus B73 identified 1,863 O2-modulated genes (Figure 1A and Supplemental Data Set
542 1). This number resembles that of DEGs previously identified by RNA-Seq in a W22 $o2$ mutant
543 versus W22 (Li et al., 2015) and in W64Ao2 versus W64A (Zhang et al., 2016). However,
544 comparison of the DEGs we identified versus the four previously published DEG sets (Hunter et
545 al., 2002; Frizzi et al., 2010; Jia et al., 2013; Zhang et al., 2016) showed little overlap, with only
546 six commonly detected DEGs (Supplemental Text 2 and Supplemental Figure 2). This
547 discrepancy can be attributed to at least two reasons. First, as has been previously shown, O2
548 may modulate partially overlapping sets of genes depending on the genetic background (Bernard
549 et al., 1994), which can be affected by the nature of *o2* mutant allele (Jia et al., 2007). Second, as
550 suggested by our temporal expression assays, the extent of dysregulation of a given O2-
551 modulated gene in *o2* versus WT depends on developmental staging; therefore, each of the
552 previous studies might have detected a distinct set of O2-modulated genes due to the specific
553 stages selected for analysis (ranging from 15 to 25 DAP).

554 Our ChIP-Seq analysis detected 6,365 putative O2-bound genomic regions associated with 3,282
555 genes (Supplemental Data Set 2). Among the putative O2-bound genes, 186 were detected as
556 direct target genes of O2 based on their differential expression in WT versus *o2* backgrounds
557 (Supplemental Data Set 3). Of these, we detected 13 of the 35 O2-activated direct target genes
558 identified by Li et al. (2015) (Supplemental Figure 14 and Supplemental Data Set 9). Compared
559 to this previous study, our ChIP-Seq and RNA-Seq analysis also identified 134 additional O2-
560 activated direct targets, including six 22-kD α -zein genes, the *LKR/SDH* gene, and the *O2* gene
561 itself (Supplemental Data Set 9), which were previously identified as canonical targets of O2
562 based on EMSAs, DNase I footprinting, ChIP-quantitative PCR, *in vivo trans*-activation assays,
563 and/or differential mRNA/protein accumulation in an *o2* mutant versus WT (Schmidt et al., 1990;
564 Lohmer et al., 1991; Schmidt et al., 1992; Kemper et al., 1999; Locatelli et al., 2009).

565 The GO term enrichment and metabolic pathway analyses of O2-modulated and/or bound gene
566 sets revealed that O2 likely regulates storage-protein gene expression and the associated amino
567 acid synthesis/metabolism processes both directly and indirectly (Figures 2 and 3; Supplemental
568 Data Set 4). The varied extent of downregulation of the different zein gene families/sub-families
569 in *o2* is consistent with the previous studies of zein mRNA and/or protein levels in the mutant
570 (Kodrzycki et al., 1989; Zhang et al., 2015; Yang et al., 2016), supporting the notion that distinct
571 zein gene families are regulated by diverse gene regulatory mechanisms, and these likely involve
572 combinatorial activities of O2 and other endosperm-expressed TFs. In addition, our analyses
573 provide evidence that the regulation of carbohydrate and lipid synthesis/metabolism is primarily
574 an indirect effect of O2's regulatory function.

575 The analysis of the overlaps between O2-modulated and/or bound gene sets and the temporally
576 upregulated gene sets we identified previously (Li et al., 2014) revealed a tightly linked timing of
577 activation between *O2* and O2 targets, and also detected a number of targets that are likely
578 activated before activation of *O2* itself (Figure 4A). Accordingly, our temporal real-time
579 expression assays of *o2* versus WT endosperm identified at least two distinct modes of gene
580 activation by O2, with three distinguishable periods of gene regulatory functions associated with
581 endosperm development. The two modes differ most dramatically in the early (by ~12 DAP) and
582 mid (~12 to 18 DAP) developmental periods. In the first mode, the activation of the O2 targets at
583 the early period is likely dependent on the expression of O2 (Figures 4C to 4F), whereas in the

second mode, O₂ is not required for the activation of the O₂ targets at the early period, but is likely required for the maintenance of their expression at the mid period (Figures 4G to 4M). In both cases, there are likely additional regulators that can activate O₂ target-gene expression in an O₂-independent manner during the late period, which begins at about 18 to 22 DAP (Figures 4C to 4M). The nature of the TFs regulating the early activation of O₂ target genes remains unclear, but this program is likely involved in establishing the initial active state of the target genes with or without O₂. Once activated, another set of regulators seems to be required for the maintenance of the high level of expression of the O₂ network genes in the subsequent periods. These regulators likely include, in addition to O₂ itself, the TFs that co-regulate target genes with O₂ (*e.g.*, bZIP17) and/or the TFs that are encoded by O₂ target genes acting downstream of O₂ (*e.g.*, NKD2). Interestingly, the expression of such regulators may be initiated early in endosperm development in an O₂-independent manner, but their continued high expression could be dependent on O₂ (Figures 4H and 4M). Moreover, these factors might not be necessarily expressed in an endosperm-specific manner during the plant life cycle (Figure 5). The distinct behavior of O₂-network genes during the mid and late periods—that is, the significant downregulation of O₂ target genes in the mid period and a near but not complete recovery of expression in the late period—is likely dictated by the requirement of O₂ in the mid period and a partial requirement of O₂ in the late period. The latter could be due to a partial compensation or redundancy displayed by otherwise non-endosperm-specific bZIP proteins in the absence of the endosperm-specific O₂. Together, although our data do not allow us to determine whether O₂ binds the direct target genes (detected at 15 DAP) during all the analyzed stages of endosperm development, the temporal expression patterns suggest that the O₂ GRN is modulated finely, based on the period of endosperm development. However, it is also possible that post-transcriptional regulatory mechanisms may also contribute to the modulation of the encoded gene products as mRNA accumulation patterns do not correlate strictly with the respective protein levels for many endosperm genes (Walley et al., 2013). Therefore, further understanding of the O₂ network will require comprehensive temporal analyses of gene expression programs, using both transcriptomic and proteomic approaches, and genome-wide DNA-binding patterns of O₂ and its target genes throughout endosperm development.

O₂ has long been identified as a transcriptional activator, but there was little prior evidence to suggest that O₂ also functions as a direct transcriptional repressor. In our analysis, we detected

615 839 putative O2-repressed genes, including 39 direct targets. The O2-repressed direct target gene
616 set showed temporally upregulated patterns throughout endosperm development (Supplemental
617 Figure 6), suggesting that O2 represses these genes quantitatively to a certain degree, but does
618 not seem to affect their otherwise global and temporally upregulated expression pattern in WT.
619 These RNA-Seq-based observations are further supported by our temporal RT-qPCR analysis of
620 individual genes. For instance, two of the O2-repressed direct targets examined in our temporal
621 analysis (GRMZM2G443668 and GRMZM2G034623) showed upregulated expression patterns
622 in both B73 and B73 α 2 endosperm (Supplemental Data Set 8). As discussed above, it is yet to be
623 determined if these genes are bound by O2 at the later developmental stages, and thus it is
624 unclear if the upregulation of mRNA levels in the α 2 mutant is due to loss of direct
625 transcriptional repression by O2. In addition, it is possible that at least a subset of the putative
626 O2-repressed genes were detected as a result of proteome rebalancing processes in the α 2 mutant
627 endosperm rather than as a result of loss of repression by O2—that is, their mRNA levels could
628 be elevated in the α 2 endosperm as part of an overall increase in the levels of non-zein mRNAs
629 to enhance synthesis of non-zein proteins (Wu and Messing, 2014; Larkins et al., 2017).
630 Nevertheless, these data strongly suggest O2 functions as both an activator and a repressor.
631 Our *cis*-motif analysis of O2-bound genomic regions revealed centrally-enriched bZIP-like
632 binding motifs, which likely act as *cis*-regulatory sequences for O2 and related bZIP TFs (Figure
633 1F). In fact, the conserved sequence of the two bZIP-like motifs (CCACGTCA) was essentially
634 identical to the O2-binding motif identified by Li et al. (2015) that exhibited strong binding to
635 the O2 protein in an EMSA. Our analysis of *cis*-motifs (Supplemental Table 4) supports a role
636 for additional storage program regulators in association with the O2-regulated gene network. The
637 identification of many TF genes, including several bZIP genes, as direct targets of O2 provides
638 novel insight into the complexity of the O2 GRN. The *bZIP17* gene, which is a paralog of *O2*,
639 was identified as a direct target of O2 based on our ChIP-Seq and RNA-Seq analysis, and the
640 bZIP17 protein can interact with O2 to co-activate zein-gene expression in DLR assays. This
641 suggests O2 and bZIP17 could form a coherent feed-forward loop—that is, the output (activation
642 or repression) of direct regulation (*e.g.*, O2 directly activates *FL2*) is the same as the overall
643 output of indirect regulation (*e.g.*, O2 indirectly activates *FL2* through activation of *bZIP17*)
644 (Mangan and Alon, 2003)—in control of some of O2-regulated genes (Figure 6; Supplemental
645 Data Set 3). Furthermore, these data indicate that bZIP17 is a putative novel regulator of the

646 endosperm storage program and could play redundant roles with the O2/OHP proteins. Notably,
647 the co-activation of only one of the six tested O2 peaks by O2 and bZIP17 (Figure 6B;
648 Supplemental Table 5) and, similarly, the co-activation of only three of the six O2 peaks by O2
649 and NKD2 (Figure 7B; Supplemental Table 7), suggest that the specialized roles of other TFs in
650 co-activating a unique subset of direct O2 target genes with O2 could underlie the complexity of
651 the O2 regulatory network. Alternatively, the lack of co-activation of several O2 direct target
652 gene-associated peaks by O2 and bZIP17 (or NKD2) in *N. benthamiana*—assuming that the
653 associated genes are co-activated by O2 and bZIP17 (or NKD2) *in vivo*—might reflect the
654 possibility that binding sites of bZIP17 (or NKD2) are localized outside the O2 peak regions. In
655 such cases, O2 and bZIP17 would be co-activating the same gene by binding different *cis*-motifs,
656 rather than in the form of heterodimers.

657 Interestingly, our DLR assays show O2 and NKD2 co-activate *bZIP17* (Figure 7B), indicating a
658 potential role for bZIP17, in combination with O2 and the NKDs, in regulation of endosperm cell
659 differentiation. In addition, detection of two stress-responsive bZIP genes—*LIP15* and *GBF1*—
660 as direct O2 targets suggests O2 controls responses to low temperature and hypoxia through
661 direct regulation of these TF genes (Supplemental Data Set 3); coincidentally, the GO term
662 enrichment analyses indicate the O2-activated indirect targets are enriched for biological
663 processes related to abiotic stress responses (Figure 2B). Furthermore, because each bZIP TF has
664 the potential to dimerize with certain other bZIPS and to co-regulate target genes, the O2-
665 regulated bZIP genes remain to be further characterized for interaction at the protein level and
666 for target-gene co-activation activities, in order to further understand the O2/bZIP-regulated gene
667 network and the roles of the bZIP proteins in the regulation of endosperm development.

668 *O2* is directly regulated by NKD1 and NKD2 based on downregulation of *O2* mRNA in 15-DAP
669 aleurone of a *nkd1;2* double mutant and *trans*-activation of an *O2* promoter by NKD1 and NKD2
670 individually in DLR assays performed with aleurone protoplasts (Gontarek et al., 2016). Our data
671 indicate *NKD2* is directly activated by O2 in the endosperm and the NKD2 protein can co-
672 activate target genes with O2, potentially forming another set of coherent feed-forward loops
673 within the O2 network (Figures 7A to 7C; Supplemental Data Set 3). Moreover, our enrichment
674 analyses of O2-modulated and/or bound gene sets versus previously reported endosperm cell-

675 type-specific gene sets (Zhan et al., 2015) indicates aleurone cell differentiation could involve
676 the activity of the O2-regulated gene network (Figure 7E).

677 Interestingly, our analysis detected *VP1* as being indirectly activated by O2 ($\log_2\text{FC} = -2.10$;
678 Supplemental Data Set 1). *VP1* has been shown to function in regulation of seed germination
679 through direct or indirect repression of germination-specific aleurone α -amylase genes (Hoecker
680 et al., 1995, 1999), but an earlier role for *VP1* in aleurone cell differentiation has not yet been
681 reported. Furthermore, *VP1* itself is directly activated by N KD1 and N KD2 (Gontarek et al.,
682 2016). Considering these observations, we hypothesize O2, bZIP17, N KD1, N KD2, and *VP1* co-
683 regulate a complex gene network associated with a set of endosperm developmental functions,
684 including cell differentiation, storage, maturation, responses to abiotic stresses, and the seed
685 germination programs (Figure 8). In support of this model, our LCM-based transcriptome
686 analysis of the 8-DAP kernel detected spatially overlapping expression patterns of all these TF
687 genes, with all of them showing relatively moderate levels of expression in the aleurone (FPKM
688 ≥ 2.12), while the *O2*, *bZIP17*, *N KD1*, and *N KD2* genes were also expressed in central starchy
689 endosperm and conducting zone (FPKM ≥ 0.80) (Figure 7D) (Zhan et al., 2015). However,
690 downregulation of *O2* mRNA was detected only in the aleurone, but not in starchy endosperm of
691 the *nkd1;2* double mutant (Gontarek et al., 2016), indicating distinct roles of O2 and N KDs in
692 aleurone versus starchy endosperm. Therefore, a spatial (and temporal) analysis of gene activities
693 in endosperm cell types of single mutants and higher order mutant combinations of O2, bZIP17,
694 N KDs, and/or *VP1* are necessary to fully understand the GRNs controlled by these TFs.

695

696 METHODS

697 Plant Materials and Growth

698 The *Zea mays* B73o2 inbred line was obtained from Seth Murray (Texas A&M University) and
699 was likely originally developed by Peter Loesh and colleagues by backcrossing an *o2* allele from
700 a W22 background into B73. The B73o2 seeds have been deposited at the Maize Genetics
701 Cooperation Stock Center (Stock number: 701D o2^B73). To confirm the *o2* mutation in the
702 B73o2 mutant, we examined the kernel phenotype of B73o2 in comparison to a W22o2, a
703 W64Ao2, and the reciprocal F1 seeds obtained from crosses among B73o2, W22o2, and

704 W64Ao2. Similar to the inbred mutants, 100% of the mature kernels produced by all reciprocal
705 crosses showed an opaque phenotype (Supplemental Figure 1A). The failure of complementation
706 among all three *o2* alleles confirmed the presence of an *o2* mutation in the B73_{*o2*} mutant line
707 used in our analyses. To confirm the nature of the *o2* mutant sequences in the B73_{*o2*} inbred used
708 in our studies, we cloned and sequenced the *O2* gDNA in B73_{*o2*} in comparison to W22_{*o2*}. A
709 2,711-bp sequence spanning 154 bp upstream of the start codon to 11 bp downstream the stop
710 codon (based on gene model annotation in B73) were obtained for B73_{*o2*}; and a 2,714-bp
711 sequence spanning from 154 bp upstream the start codon to 14 bp downstream the stop codon,
712 were obtained for W22_{*o2*}. These two sequences are 100% identical within the 2,711 bp covered
713 by the B73_{*o2*} sequence, indicating the *o2* alleles in B73_{*o2*} and W22_{*o2*} mutants are of the same
714 origin. Alignment of the 2,711-bp sequence with *O2* genomic sequence in B73 using SnapGene
715 v4.0.5 (from GSL Biotech; available at snapgene.com) detected 39 mismatches and 23 gaps,
716 whereas alignment of the same sequence with the *O2* genomic sequence in W22 detected 32
717 mismatches and 21 gaps. In both alignments, many mismatches and gaps were found in both
718 exonic and intronic sequences, including many missense mutations and insertions/deletions in
719 the CDS regions (Supplemental Figure 1B). An online BLASTN search against the NCBI nr
720 nucleotide database (accessed July 2017) using the 2,711-bp sequence showed that the most
721 similar WT gene is the *O2* gene in the maize accession Ac 1503 GM 1407 (X15544.1; with 34
722 mismatches and 23 gaps, based on subsequent SnapGene alignment), whereas the most similar
723 mutated gene is the *O2* gene in the quality protein maize (QPM) inbred line CA339 (KF831426.1;
724 with 3 mismatches) (Maddaloni et al., 1989; Chen et al., 2014b). Because a modest level of *O2*
725 mRNAs were detected in B73_{*o2*} endosperm at stages beyond 10 DAP (Figure 4B), and to
726 confirm that the *O2* mRNAs detected by RT-qPCR in the mutant were derived from the mutated
727 *O2* gene, we sequenced the *O2* cDNA in 22-DAP mutant endosperm and obtained a 2,675-bp
728 sequence spanning 105 bp upstream the start codon to 14 bp downstream the stop codon. The
729 putative coding sequence within this 2,675 bp was 100% identical to the *O2* gDNA in B73_{*o2*},
730 with five gaps corresponding to the five introns in the annotated gene model of *O2* in the B73
731 genome (Supplemental Figure 1B). Immunoblot assays using the anti-O2 antibody detected
732 accumulation of the O2 protein at a relatively high level by 15 DAP in the WT but no
733 accumulation in the B73_{*o2*} mutant (Supplemental Figures 1C to 1E).

734 Maize plants used for RNA-Seq, ChIP-Seq, RT-qPCR, immunoblot, and *O2* gene/cDNA
735 sequencing experiments were grown in a greenhouse at University of Arizona with 30°C/25°C
736 (day/night) temperature cycles under natural light supplemented with high pressure sodium and
737 metal halide lamps for 16 h per day. The endosperm tissues for the RNA-Seq and ChIP-Seq
738 experiments were manually dissected from 15-DAP kernels obtained from self-pollinated B73
739 and B73o2 plants grown during June to October 2012. The tissues for the RT-qPCR assays (and
740 sequencing of the *O2* cDNA in B73o2) were manually dissected from self-pollinated B73 and
741 B73o2 plants grown during November 2013 to February 2014. For these experiments, each
742 biological replicate of a given sample included multiple endosperms from a single ear (plant).
743 Biological replicates 1 and 2 of each ChIP-Seq sample were derived from the same ear as
744 biological replicates 1 and 2 of each RNA-Seq sample, respectively. Leaf tissues were collected
745 from B73o2 and W22o2 mutants around one week after germination. After their seeds were
746 stratified at 4°C for 2 days, the *N. benthamiana* plants were grown in a growth chamber at 22°C
747 with 16-h light per day.

748 **Immunoblot assays**

749 Nearly 100 mg of endosperm tissue was ground to a fine powder with liquid nitrogen and then
750 homogenized in 200 µl of protein extraction buffer [1% SDS, 100 mM Tris-Cl (pH 7.5), 100 mM
751 NaCl, 5 mM EDTA] supplemented with 2% β-mercaptoethanol. The homogenate was
752 centrifuged at 12,000× g at 4°C for 15 min. About 10 µl of supernatant was mixed with 6× SDS-
753 PAGE loading buffer and heated at 95°C for 5 min prior to analysis by SDS-PAGE. After
754 separation, the proteins were blotted onto a nitrocellulose membrane (Sigma-Aldrich) using the
755 Owl HEP-1 Semi Dry Electroblotting System (Thermo Scientific) and probed with an anti-O2
756 antibody using the AmershamTM ECLTM Select Western Blotting Detection Reagent (GE
757 Healthcare Life Sciences) following the manufacturer's instructions. The membrane was then
758 exposed to X-ray film (BioExpress) to detect specific proteins.

759 **RNA-Seq**

760 Approximately 4 µg of total RNA was isolated from each of six endosperm samples (2
761 genotypes × 3 replicates) using an SDS-phenol method previously described (Li et al., 2014) and
762 quality-checked using an Agilent 2100 Bioanalyzer (Agilent Technologies). Using a TruSeq
763 DNA Sample Preparation Kit v2 (Illumina), polyA-containing mRNAs were purified,

764 fragmented, and reverse-transcribed at the University of Arizona Genetics Core facility and used
765 to construct multiplexed RNA-Seq libraries. The resulting libraries were sequenced on a single
766 flow cell lane of an Illumina HiSeq2500 platform at this facility using a TruSeq SBS kit
767 v3 (Illumina) to produce 2× 100-nucleotide paired-end reads.

768 **ChIP-Seq**

769 Chromatin purification was performed following a previously published protocol (Saleh et al.,
770 2008) with minor modifications. Dissected endosperms were cross-linked (fixed) using 1%
771 formaldehyde in phosphate buffer (10 mM Sodium Phosphate, 50 mM NaCl, 0.1 mM Sucrose,
772 pH 7.0) with vacuum infiltration for 30 min. Fixation was quenched with 125 mM glycine, and
773 the fixed materials were washed three times with distilled water, partially dried with paper
774 towels, frozen in liquid nitrogen, and stored at -80°C. About 2 g of the fixed tissue was ground to
775 fine powder in liquid nitrogen and homogenized in 25 ml of extraction buffer 1 [0.4 M Sucrose,
776 10 mM Tris-Cl (pH 8.0), 10 mM MgCl₂, 5 mM β-mercaptoethanal]. The homogenate was then
777 filtered through two layers of Miracloth (Calbiochem-Novabiochem Corporation), after which it
778 was centrifuged at 12,000× g for 10 min at 4°C. After removing the supernatant, the pellet was
779 resuspended in 5 ml of extraction buffer 2 [0.25 M Sucrose, 10 mM Tris-Cl (pH 8.0), 10 mM
780 MgCl₂, 1% Triton X-100, 5 mM β-mercaptoethanal] and centrifuged as described above. The
781 pellet was resuspended in 0.3 ml extraction buffer 3 [1.7 M Sucrose, 10 mM Tris-Cl (pH 8.0), 2
782 mM MgCl₂, 0.15% Triton X-100, 5 mM β-mercaptoethanal] and carefully layered onto 0.3 ml of
783 extraction buffer 3, and centrifuged at 16,000× g at 4°C for 1 h. The resulting pellet (chromatin)
784 was sonicated as described below. Solutions for chromatin purification contained fresh 1 mM
785 PMSF and 1× Protease inhibitor cocktail (Thermo Scientific Company LLC).

786 ChIP was performed using a ChIP Assay Kit (Millipore Corporation, Billerica, MA) following
787 the manufacturer's instructions with modifications. The chromatin pellet from 1 g of tissue was
788 resuspended in 1 ml of immunoprecipitation buffer [0.1% SDS, 1% Triton X-100, 2 mM EDTA,
789 20 mM Tris-Cl (pH 8.0), 150 mM NaCl], with 1× Protease inhibitor cocktail and 1 mM PMSF
790 freshly added), and sonicated in 0.25-ml aliquots with a probe sonicator (Fisher Scientific Model
791 120 Sonic Dismembrator) for six cycles of 20 s at 25% amplitude and cooled in ice water for 40
792 sec between pulses. The sonicated chromatin was centrifuged at 16,000× g for 10 min at 4°C and
793 the supernatant was used for immunoprecipitation. A 10 µl aliquot from 1 ml of supernatant (1%)

794 was saved as “input” DNA. The chromatin solution was pre-cleared using 60 µl of protein A
795 agarose/Salmon Sperm DNA (50% Slurry; Upstate) for 1 h at 4°C on a rotating Labquake tube
796 shaker. The mixture was then centrifuged at 13,800× g at 4°C for 1 min. The supernatant was
797 mixed with 5 µl anti-O2 antibody and incubated overnight at 4°C on a rotating tube shaker. Sixty
798 µl of protein A agarose/Salmon Sperm DNA (50% Slurry) was added to the mixture and then
799 incubated for 2 h at 4°C on a rotating tube shaker. The agarose beads were pelleted using a
800 microfuge at 82× g for 1 min at 4°C and the supernatant was carefully removed. The beads were
801 washed and eluted following the manufacturer’s instructions. The eluate and the “input” fraction
802 were reverse-cross-linked by heating at 65°C for overnight and the DNA was purified by using
803 Zymo ChIP DNA Clean & Concentrator (Zymo Research). The ChIPed DNA was eluted with 10
804 µl Elution Buffer, and quality-checked using an Agilent 2100 Bioanalyzer. Using an Illumina
805 Pico DNA Seq Library Preparation Kit (Gnomegen Inc.), nearly 10 ng of purified ChIPed DNA
806 from each endosperm sample (2 genotypes × 2 replicates) was used by the University of Arizona
807 Genetics Core facility to generate a set of multiplexed ChIP-Seq libraries following the
808 manufacturer’s instructions. The resulting libraries were sequenced on a single flow cell lane of
809 an Illumina HiSequation 2500 platform at the same facility to produce 2× 100-nucleotide paired-
810 end reads.

811 **Analysis of RNA-Seq and ChIP-Seq data**

812 Raw reads from RNA-Seq and ChIP-Seq were trimmed to remove adapter sequences and low-
813 quality bases using the Trimmomatic program (Bolger et al., 2014) with the parameter
814 TRAILING set to three. The resulting RNA-Seq reads were mapped to the maize reference
815 genome (B73 RefGen_v3) using Tophat v2.0.9 (Trapnell et al., 2009) with parameters previously
816 reported (Zhan et al., 2015). Reads mapped to each gene were counted using the multicov
817 function of BEDTools v2.17.0 (Quinlan and Hall, 2010) and normalized using the R package
818 edgeR v3.2.4 (Robinson et al., 2010) with the trimmed mean of M-values method. Genes with
819 raw counts per million (CPM) > 1 in at least 3 samples were tested for differential expression
820 analysis using edgeR with an exact test analogous to Fisher’s exact test. FDR < 0.05 was used as
821 the cutoff to call DEGs. The trimmed ChIP-Seq reads were mapped to the reference genome
822 using Bowtie v2.1.0 (Langmead and Salzberg, 2012) with the following parameters: --score-Min
823 L, -0.6, -0.18 --end-to-end --very-sensitive --no-discordant. Mapped reads for duplicates of the

824 B73 samples and the B73o2 samples (control) were merged, respectively, and were used for
825 peak-calling using MACS v2.1.0.20140616 (Zhang et al., 2008; Feng et al., 2012) with the
826 following parameters: -g 2.06e9 -q 0.01 -mfold 10 30. ChIP-Seq read coverage across the
827 genome was visualized using the Integrative Genomics Viewer (Thorvaldsdottir et al., 2013).
828 The “slop” and “intersect” functions of BEDTools were used to determine gene-peak association
829 to identify O₂-bound genes. Information about maize genome annotation and gene functional
830 description were obtained from Ensembl Plants (plants.ensembl.org, release 19) and MaizeGDB
831 (maizegdb.org) (Andorf et al., 2016). Annotation of TFs was obtained from Plant Transcription
832 Factor Database v3.0 (Jin et al., 2014) and GrassTFDB of GRASSIUS (Gray et al., 2009; Yilmaz
833 et al., 2009). Annotation of zein genes was curated based on the information summarized by
834 Chen et al. (2014). The GO term annotations for maize genes were obtained from Gramene
835 (gramene.org, release 40) and the agriGO database v1.2 (Du et al., 2010). GO term enrichment
836 analysis was performed using Blast2GO v3.0.11 (Gotz et al., 2008). Metabolic pathway
837 association analysis was performed using CornCyc v8.0 (Walsh et al., 2016) on MaizeGDB.
838 Putative functions for genes of interest that lacked functional annotations were inspected by
839 BLASTX search of the NCBI nr and Swissprot databases (accessed September 2017) as
840 described previously (Zhan et al., 2015). A customized Perl script was used to detect the
841 presence of previously reported O₂-binding sites [the 4-bp core sequence associated with the
842 *Starch synthase III (SSIII)* gene was excluded because it is present in nearly all (91.4%) of the
843 5'-regulatory sequences in the B73 genome] within the 5'-regulatory regions of O₂-modulated
844 and/or bound genes, which we defined as 1 kb upstream and 0.5 kb downstream of the annotated
845 transcription start sites. MEME-ChIP v4.9.1 was used for *cis*-motif enrichment analysis, and the
846 JASPAR 2014 Plantae motif database (Mathelier et al., 2014) was used for motif comparison by
847 TOMTOM.

848 **BLAT**

849 The available sequences of microarray probes or cDNAs were aligned to the B73 cDNA
850 sequences (obtained from Ensembl Plants) using BLAT v34x10 (Kent, 2002) to identify the
851 corresponding genes in the B73 genome. The best alignment (based on matches) for each
852 probe/cDNA was selected using a customized Perl script. The alignments with identity < 80%
853 were manually excluded.

854 **Expression of GST fusions in *Escherichia coli* and their purification**

855 The open reading frame (ORF) of *O2* (GRMZM2G015534_T02) was amplified with primers
856 O2T2PGEX-FXba (5'-GCCTCTAGACATGGAGCACGTATCTCAATG-3') and
857 O2T2PGEX-RHind3 (5'-GCCAAGCTTCTAACATACATGTCCATGTG-3'), digested with XbaI
858 and HindIII, and cloned into the XbaI and HindIII sites of the pGEX-KG-Kan vector. This
859 construct, called O2-pGEX-KG-Kan, was introduced into *E. coli* strain ArcticExpress Blue
860 (Agilent Technologies). For protein production, cells were grown in Superbroth containing 50
861 µg/ml kanamycin at 37°C to an OD₆₀₀ of 0.6 and then cooled to 30°C. Gene expression was
862 induced with 0.05 mM IPTG and the cells were grown at 30°C for 3 hours following induction.
863 For protein purification, induced cells were centrifuged, and the pellet was frozen and thawed,
864 resuspended in lysis buffer [10 mM Tris (pH 8.0), 10 mM EDTA, 10 mM NaCl] containing 500
865 µg/ml lysozyme, incubated at room temperature for 30 minutes, and then sonicated to reduce
866 viscosity. The sonicated cells were centrifuged, and the supernatant was collected and then
867 passed through a 0.45 µm filter. O2 protein was purified using a 1 ml glutathione sepharose
868 column (GSTrap FF, GE Healthcare) following the manufacturer's instructions. Purification of
869 GST protein was similar, except that gene expression was carried out at 37°C for 1 hour.

870 **EMSA**

871 All EMSA probes were labeled with Cy5 and generated by PCR amplification from pCRII-
872 TOPO clones using Cy5-labeled M13 forward and reverse primers. For the bZIP17 clone, two
873 80-nt oligonucleotides were annealed as described below. For all other clones, the sequences of
874 interest were amplified from the B73 genome by PCR using the primers listed in Supplemental
875 Table 8. All inserts were ligated into the pCRII-TOPO vector using the TOPO TA Cloning kit
876 (Fisher Scientific). Unlabeled competitors were prepared by annealing oligonucleotides of 25 to
877 50 nt in length. The sequences of the oligonucleotides are listed in Supplemental Table 9.
878 Annealing of oligonucleotides was performed as follows: 1 nmol of each oligonucleotide was
879 mixed in binding buffer, heated to 95°C in a thermal cycler and cooled slowly to room
880 temperature. Binding buffer consisted of 10 mM Tris (pH 7.5), 50 mM KCl, 1 mM DTT, and 0.1%
881 Tween 20. All binding reactions were carried out at room temperature for 20 minutes in a total
882 volume of 20 µl containing binding buffer; 2.5% glycerol; 25 nM probe; and 13 nM, 38 nM, or
883 115 nM O2 protein. GST protein at 100 nM was included as a control. Binding reactions

884 containing competitor DNAs contained 115 nM O2 protein and 500 nM or 5 μ M competitor
885 DNA. Reaction products were separated by gel electrophoresis using 1% agarose in 0.5 \times TBE
886 and scanned on a GE Typhoon FLA9500.

887 **RT-qPCR**

888 RT-qPCR assays were performed with a time series of endosperm material collected at 6, 8, 10,
889 12, 15, 18, 22, and 30 DAP from B73 and B73o2 with three biological replicates. RNA isolation,
890 cDNA synthesis, and qPCR experiments were performed essentially as described previously
891 (Wang et al., 2010; Li et al., 2014) using the primers listed in Supplemental Table 10. The raw
892 threshold cycle (Ct) values were normalized against the Ct values of the *Thioredoxin (TXN)* gene,
893 which showed a similar and stable expression in B73 versus B73o2 at all the analyzed stages
894 (Supplemental Data Set 8). The normalized Ct values were manually cut off at 36. The relative
895 difference (*i.e.*, -log₂FC) in mRNA levels of a gene between B73 and B73o2 at a given stage was
896 determined as: $\Delta\Delta Ct = Ct_{B73o2} - Ct_{B73}$, where both Ct_{B73o2} and Ct_{B73} are normalized Ct values.

897 **Amplification and sequencing of O2 genomic DNA and cDNA**

898 Maize genomic DNA (gDNA) was isolated from leaf tissues using a urea-based method as
899 described previously (Holding et al., 2008). Each biological replicate of a given leaf sample
900 included about 20 mg of leaf tissue from a single plant. Using the same pair of primers, 5'-
901 TTAACTCATGGGTGCATAGAGA-3' and 5'-GAAACCCGCAGTGCCTAATA-3', the *O2*
902 gene sequence was amplified from leaf gDNA of B73o2 and W22o2 (3 and 2 biological
903 replicates, respectively), while the *O2* cDNA was amplified from a 22-DAP endosperm cDNA
904 sample from B73o2 (2 biological replicates) by PCR using the Phusion Hot Start II DNA
905 Polymerase (Fisher Scientific). The PCR products from gDNA amplification were cloned into
906 the pGEM-T vector (Promega) and were Sanger-sequenced using the vector-specific M13F(-21)
907 and M13R Reverse primers and the gene-specific primers 5'-ATCTTTATTATTCCCTCGCT-3'
908 and 5'-GCTCTCAGCACCCCTGTTGTC-3'; the PCR products from cDNA amplification were
909 Sanger-sequenced directly using the same primers as used for PCR and primer 5'-
910 TCAAGAGCCTGCATCCAT-3'.

911 **Phylogenetic analysis**

912 Protein sequences of bZIP family members were obtained from Ensembl Plants, and the longest
913 annotated protein sequence encoded by each gene was selected for phylogenetic analysis using a
914 customized Perl script. Multiple sequence alignment was performed using Clustal Omega (v1.2.4;
915 <https://www.ebi.ac.uk/Tools/msa/clustalo/>) (Sievers et al., 2011). The alignment is provided as a
916 text file in Supplemental File 1. A phylogenetic tree based on the alignment was inferred using
917 RAxML v8.0.23 (Stamatakis, 2014) with the maximum likelihood method using a Whelan and
918 Goldman (WAG) model of amino acid evolution (Whelan and Goldman, 2001) and a Gamma
919 model of rate heterogeneity. The confidence level of nodes in the tree was determined by
920 inferring phylogeny in 100 bootstrap replicates. The tree was visualized using FigTree v1.4.3
921 (tree.bio.ed.ac.uk/software/figtree/).

922 ***In vitro* pull-down assay**

923 The full-length ORF corresponding to each protein was PCR-amplified from a 15-DAP B73
924 endosperm cDNA (O2) or a clone from the GRASSIUS maize TFome collection (bZIP17; clone
925 pUT6435) (Burdo et al., 2014) and cloned into pGBKT7 and pGADT7 vectors, allowing the
926 protein to be expressed as fusion protein with an HA tag or a c-Myc tag. The primers and
927 restriction enzymes used to generate the clones are listed in Supplemental Table 11. Using the
928 resulting constructs as templates, tagged proteins were synthesized *in vitro* with [³⁵S]methionine
929 (PerkinElmer) using the TnT® Quick Coupled Transcription/Translation Systems (Promega)
930 following the manufacturer's instructions. The *in vitro* pull-down assays were performed as
931 previously described (Cifuentes-Rojas et al., 2011) with minor modifications. Briefly, for a given
932 pair of assayed proteins, the TnT-produced proteins (10 µl each) were mixed, incubated at 30°C
933 for 20 min, and then at 4°C for 20 min while turning on a tube rotator. Subsequently, 300 µl of
934 blocking buffer (buffer W-100 [20 mM TrisOAc (pH 7.5), 10% glycerol, 1 mM EDTA, 5 mM
935 MgCl₂, 0.2 M NaCl, 1% NP-40, 0.5 mM sodium deoxycholate, and 100 mM potassium
936 glutamate] containing 0.5 mg/ml BSA, 0.5 mg/ml lysozyme, 0.05 mg/ml glycogen, and 1 mM
937 DTT) was added and the mixture was incubated at 4°C for 1 hour while rotating. The anti-Myc
938 agarose (Sigma Aldrich) was blocked 3 times (15 min each) in 1 ml blocking buffer at 4°C while
939 rotating. The blocked protein mixture was mixed with anti-Myc agarose, incubated at 4°C for 2
940 hours while rotating, and then centrifuged at 2,500× g for 1 min at 4°C. The supernatant was
941 saved as “input” protein, while the precipitated agarose beads were washed 5 times with 1 ml W-

942 300 buffer (W-100 containing 300 mM potassium glutamate) and proteins were eluted by adding
943 25 µl 5× SDS-PAGE sample buffer. Twenty µl of the pulled-down fraction, along with
944 approximately 6% of the “input” fraction, were resolved by SDS-PAGE in 10% acrylamide and
945 visualized using a storage phosphor screen GP (Kodak) and a Storm 860 molecular imager
946 (Molecular dynamics).

947 **BiFC assay**

948 The wild-type *O2* ORF was PCR-amplified from a 15-DAP B73 endosperm cDNA; the mutated
949 *O2* ORF (named O2LA), which encodes an *O2* protein with two leucine residues in the leucine-
950 zipper domain substituted by alanine residues (L265A and L272A), was generated using a PCR-
951 based site-directed mutagenesis method. The attB adapter PCR method (Gateway Technology,
952 Invitrogen) was used to generate full attB PCR products. The attB PCR products were cloned
953 into the pDONR207 vector by BP reaction to generate entry clones for *O2* and O2LA, while the
954 pUT6435 clone was directly used as the entry clone for bZIP17. The expression clones were
955 generated by LR reaction using pDEST-gwVYCE and pDEST-gwVYNE (Gehl et al., 2009) as
956 the destination vectors, allowing the *O2/O2LA/bZIP17* protein to be expressed as a fusion
957 protein with the C terminus (Venus^C) or N terminus (Venus^N) of the Venus YFP. The primers
958 used to generate clones for *O2* and O2LA are listed in Supplemental Table 12. All clones were
959 Sanger-sequenced to confirm the inserts. For each assayed pair of fusion proteins, leaves of 5- to
960 6-week-old *N. benthamiana* plants were co-infiltrated with two individually transformed
961 *Agrobacterium tumefaciens* strain GV3101 (pMP90)—each strain harboring one of the two
962 fusion-protein-coding constructs—and the p19 helper strain (all culture OD₆₀₀ adjusted to 0.5).
963 Leaf tissue was collected about 48 h after infiltration and fluorescence was examined using an
964 Axiophot compound epifluorescence microscope (Zeiss, Jena, Germany) as described previously
965 (Wang et al., 2006).

966 **DLR assay**

967 DLR assays for *O2*-peak binding were performed as previously described (Taylor-Teeple et al.,
968 2015) with minor modifications. The *O2* ORF was PCR-amplified from the 15-DAP B73
969 endosperm cDNA and cloned into the pDONR221-P1-P4 vector by BP reaction to generate the
970 pLAH-O2 construct; each *O2* peak region was PCR-amplified from B73 leaf gDNA and was
971 cloned into the pDONR221-P3-P2 vector by BP reaction to generate a pLAH-peak construct.

972 Multi-site LR cloning was performed using these two entry clones, along with a third entry clone
973 pLAH-R4-R3-VP64Ter, and the destination vector pLAH-LARm, to generate the expression
974 construct pLAH-LARm-O2-VP64-peak. For each peak, an expression construct containing the
975 ORF of the Citrine YFP instead of O2, named pLAH-LARm-Citrine-VP64-peak, was also
976 generated as a negative control. All clones were Sanger-sequenced to confirm the inserts. Leaves
977 of 4- to 5-week-old *N. benthamiana* plants were co-infiltrated with *A. tumefaciens* strain
978 GV3101 (pMP90) harboring an expression construct (culture OD₆₀₀ adjusted to 0.12) and the p19
979 helper strain (culture OD₆₀₀ adjusted to 0.075). Leaf tissue was collected about 42 h after
980 infiltration and the activities (luminescence) of the firefly luciferase (LUC) and the *Renilla*
981 luciferase (REN) were measured with a GloMax 20/20 Luminometer (Promega) using the Dual-
982 Luciferase Reporter Assay System (Promega) following the manufacturer's instructions. Briefly,
983 about 2.5 mg leaf tissue from a single plant was frozen in liquid nitrogen, ground using a bead-
984 beater, and lysed in 200 ul Passive Lysis Buffer. Fifty ul of Luciferase Assay Reagent II was
985 added to a 10-ul aliquot of the lysate and firefly luciferase activity was measured using a
986 GloMax 20/20 Luminometer with 10 s integration time. Firefly luciferase activity was
987 subsequently quenched by adding 50 ul of Stop & Glo Reagent, which contains *Renilla* luciferin
988 substrate, and *Renilla* luciferase activity was measured with a 10 s integration time. For each
989 peak, a ratio between LUC and REN activities (LUC/REN) was determined from the activity of
990 the pLAH-LARm-O2-VP64-peak construct. The ratio for each biological replicate was then
991 divided by the ratio determined using the pLAH-LARm-Citrine-VP64-peak construct (mean of
992 biological replicates) to calculate a fold induction; the difference between the LUC/REN ratios
993 obtained using the two expression constructs were statistically tested using the Student's *t* test.
994 For the DLR assays of target-gene co-activation by two TFs, the ORF of each TF was cloned
995 into the pBN-d35Stev vector (linearized with BamHI/KpnI) using In-Fusion cloning to generate
996 a pBN-d35Stev-TF construct to enable the expression of the TF as an intact protein. For each
997 tested peak, the corresponding Citrine-containing expression construct used in the DLR assay for
998 O2 binding was also used as the negative control, and was co-infiltrated with one or two pBN-
999 d35Stev-TF constructs in the experimental assays. The LUC/REN ratios determined from each
1000 biological replicate of the experimental assays were divided by the mean ratio determined from
1001 the corresponding negative control assay to calculate a mean fold induction. Difference between
1002 the LUC/REN ratios among all the control and experimental assays were statistically tested using

1003 one-way ANOVA with post-hoc HSD test. For the peaks that were tested in both assays shown
1004 in Figure 6 (Supplemental Table 5) and Figure 7 (Supplemental Table 7), all assays for a given
1005 peak were performed at the same time, and thus the fold-induction data (mean ± SEM) for “YFP”
1006 and “YFP+O2”, respectively, are the same in the two figures (tables). All DLR assays were
1007 performed with 5 biological replicates (derived from 5 different plants) of *N. benthamiana* leaf
1008 sample. The primers and cloning methods used to generate the clones for DLR assays are listed
1009 in Supplemental Table 13.

1010

1011 **Accession Numbers**

1012 Sequence data for the wild-type genes cited in this article can be found in the Gramene database
1013 or GenBank/EMBL libraries under the following accession numbers: 15-kD β -zein,
1014 GRMZM2G086294; 18-kD δ -zein, GRMZM2G100018; 27-kD γ -zein, GRMZM2G138727;
1015 ADA2, GRMZM2G177974; AGP2, GRMZM2G027955; *azs22-4*, GRMZM2G044625; *b-32*,
1016 GRMZM2G063536; *bZIP17*, GRMZM2G103647; *bZIP104*, GRMZM2G098904; *C3H48*,
1017 GRMZM2G044004; *CA5P10*, GRMZM2G440949; *cyPPDK1*, GRMZM2G306345; *cyPPDK2*,
1018 GRMZM2G097457; *FL2*, GRMZM2G397687; *FRK1*, GRMZM2G086845; *FRK2*,
1019 GRMZM2G051677; *GBF1*, GRMZM2G011932; *GCN5*, GRMZM2G046021; *HB31*,
1020 GRMZM2G026643; *HB45*, GRMZM2G126808; *LIP15*, GRMZM2G448607; *LKR/SDH*,
1021 GRMZM2G181362; *MADS47*, GRMZM2G059102; *MAS1*, GRMZM2G102183; *MYBR10*,
1022 GRMZM2G477533; *NAC78*, GRMZM2G406204; *NAC109*, GRMZM2G014653; *NAC122*,
1023 GRMZM2G430849; *NKD1*, GRMZM2G129261; *NKD2*, GRMZM5G884137; *O2*,
1024 GRMZM2G015534; *OHP1*, GRMZM2G016150; *OHP2*, GRMZM2G007063; *Orphan154*,
1025 GRMZM2G300125; *PBF*, GRMZM2G146283; *SSIII*, GRMZM2G141399; *SUS2*,
1026 GRMZM2G318780; *TAR3*, GRMZM2G141810; and *VP1*, GRMZM2G133398. The gene and
1027 cDNA sequences of *O2* in B73*o2* and W22*o2* have been deposited in GenBank under the
1028 accession numbers MH329290 and MH329291, respectively. The RNA-Seq and ChIP-Seq data
1029 reported in this article have been deposited in the Gene Expression Omnibus (GEO) database
1030 (www.ncbi.nlm.nih.gov/geo) under the accession number GSE114343.

1031

1032 **Supplemental Data**

1033 **Supplemental Figure 1.** Genetic confirmation of the B73o2 mutant.

1034 **Supplemental Figure 2.** Comparison of O2-modulated genes identified in this study and in prior
1035 studies.

1036 **Supplemental Figure 3.** Visualization of ChIP-Seq reads and peaks around 5 previously
1037 reported direct targets of O2 using the Integrative Genomics Viewer.

1038 **Supplemental Figure 4.** Comparison of putative direct O2 target genes detected using our data
1039 versus the data generated by Li et al. (2015) when applying a similar cutoff for defining O2-
1040 bound genes.

1041 **Supplemental Figure 5.** Association of the O2-modulated and/or bound gene sets with
1042 previously reported O2-binding sites.

1043 **Supplemental Figure 6.** Expression levels of the direct O2 targets in seed organs/tissues in
1044 comparison to vegetative and reproductive organs/tissues based on the available maize
1045 expression atlas (Chen et al., 2014a).

1046 **Supplemental Figure 7.** Distribution of mapped reads around the gene models of direct O2
1047 targets.

1048 **Supplemental Figure 8.** Results of EMSAs for binding of O2 to the O2 peaks or 5'-regulatory
1049 regions associated with direct O2 targets.

1050 **Supplemental Figure 9.** DLR assays for binding of O2 to the O2 peaks associated with direct
1051 O2 targets.

1052 **Supplemental Figure 10.** Enrichment of TF gene families among the O2-modulated and/or
1053 bound gene sets.

1054 **Supplemental Figure 11.** Phylogenetic relationship among all annotated bZIP-family proteins in
1055 maize.

1056 **Supplemental Figure 12.** *In vitro* interaction between O2 and bZIP17.

- 1057 **Supplemental Figure 13.** Schematic of constructs used in DLR assays for gene co-activation by
1058 two TF proteins.
- 1059 **Supplemental Figure 14.** Venn diagram of numbers of O2-activated direct targets identified by
1060 Li et al. (2015) and by this study.
- 1061 **Supplemental Table 1.** Summary of the previously reported O2-binding sites.
- 1062 **Supplemental Table 2.** Positions of EMSA probes as compared to O2 peaks.
- 1063 **Supplemental Table 3.** Results of DLR assays of O2-target gene (peak) interaction shown as
1064 fold induction values (mean \pm SEM).
- 1065 **Supplemental Table 4.** Results of MEME-ChIP analysis of the 401-bp sequences flanking the
1066 summits of peaks associated with the putative direct O2 targets.
- 1067 **Supplemental Table 5.** Results of DLR assays of target-gene (peak) co-activation by O2 and
1068 bZIP17 shown as fold induction values (mean \pm SEM).
- 1069 **Supplemental Table 6.** Putative direct O2 targets that have previously been predicted as direct
1070 NKD2 targets genes by Gontarek et al. (2016).
- 1071 **Supplemental Table 7.** Results of DLR assays of target-gene (peak) co-activation by O2 and
1072 NKD2 shown as fold induction values (mean \pm SEM).
- 1073 **Supplemental Table 8.** Sequences of the primers used to generate the EMSA probes.
- 1074 **Supplemental Table 9.** Sequences of the primers used to generate the competitor sequences in
1075 the EMSAs.
- 1076 **Supplemental Table 10.** Sequences of primers used for RT-qPCR.
- 1077 **Supplemental Table 11.** Cloning strategies and sequences of primers used for *in vitro* pull-down
1078 assays.
- 1079 **Supplemental Table 12.** Cloning strategies and sequences of primers used for BiFC assays.
- 1080 **Supplemental Table 13.** Cloning strategies and sequences of primers used for DLR assays.

1081 **Supplemental File 1.** Text file of the alignment used to generate the phylogenetic tree in
1082 Supplemental Figure 11.

1083 **Supplemental Data Set 1.** Normalized expression levels in RPKM, results of differential
1084 expression analysis, and functional annotation for genes tested for differential gene expression.

1085 **Supplemental Data Set 2.** Associated peaks and functional annotation of O₂-bound genes.

1086 **Supplemental Data Set 3.** Normalized expression levels in RPKM, associated peaks, and
1087 functional annotation of direct O₂ targets.

1088 **Supplemental Data Set 4.** GO term enrichments and pathway associations of direct and indirect
1089 O₂ target gene sets.

1090 **Supplemental Data Set 5.** BLASTX search of the O₂-repressed direct targets against the NCBI
1091 nr database (*E*-value < 10⁻⁶).

1092 **Supplemental Data Set 6.** BLASTX search of the O₂-repressed direct targets against the
1093 Swissprot database (*E*-value < 10⁻⁶).

1094 **Supplemental Data Set 7.** Putative indirect O₂ targets that have previously been predicted as
1095 direct NKD2 targets by Gontarek et al. (2016).

1096 **Supplemental Data Set 8.** RT-qPCR data in comparison to RNA-Seq data.

1097 **Supplemental Data Set 9.** O₂-bound and activated genes identified through ChIP-Seq and
1098 RNA-Seq analysis by Li et al. (2015) and/or this study.

1099

1100 **ACKNOWLEDGMENTS**

1101 We thank Robert J. Schmidt (U.C. San Diego) for providing the anti-O₂ antibody, Seth C.
1102 Murray (Texas A&M Univ.) for providing the B73o2 seeds, Rebecca S. Boston (North Carolina
1103 State Univ.) for providing the W22o2 seeds, David R. Holding (Univ. Nebraska-Lincoln) for
1104 providing the W64Ao2 and W64A seeds and information about *o2* mutant alleles, Jörg Kudla
1105 (Univ. Münster) for providing the pDEST-gwVYCE and pDEST-gwVYNE vectors, Samuel P.
1106 Hazen (Univ. Massachusetts Amherst) for providing the pLAH-R4-R3-VP64Ter and pLAH-
1107 LARm vectors, Guang Yao (Univ. Arizona) for providing the pDONR221-P1-P4 and

1108 pDONR221-P3-P2 vectors, Syed Ali Shareef (Univ. Arizona) for assistance with the cloning of
1109 the *O2* gene and cDNA, Andrew D. L. Nelson (Univ. Arizona) for advice on the *in vitro* pull-
1110 down assays, and Joanne M. Dannenhoffer (Central Michigan Univ.), and Mark A. Beilstein
1111 (Univ. Arizona) for critical reading of the manuscript. J.Z. was supported by a graduate
1112 fellowship from the China Scholarship Council and a Boynton Graduate Fellowship in Plant
1113 Molecular Biology, School of Plant Sciences, Univ. Arizona. This work was supported by the
1114 National Science Foundation Grants DBI-1261830 (to X.W. and R.Y.), IOS-0923880 (to B.A.L.,
1115 G.N.D., and R.Y.), and IOS-1444568 (to G.N.D. and R.Y.).

1116

1117 AUTHOR CONTRIBUTIONS

1118 J.Z., G.L., B.A.L., and R.Y. designed research; J.Z., G.L., C.-H.R., S.Z., A.L., and B.G.H.
1119 performed research; C.M., and X.W. contributed new reagents/analytic tools; J.Z. and R.Y.
1120 analyzed data; and J.Z., G.L., B.A.L., G.N.D., and R.Y. wrote the article.

1121

1122 REFERENCES

- 1123 Andorf, C.M., Cannon, E.K., Portwood, J.L., 2nd, Gardiner, J.M., Harper, L.C., Schaeffer, M.L.,
1124 Braun, B.L., Campbell, D.A., Vinnakota, A.G., Sribalusu, V.V., Huerta, M., Cho, K.T.,
1125 Wimalanathan, K., Richter, J.D., Mauch, E.D., Rao, B.S., Birkett, S.M., Sen, T.Z., and
1126 Lawrence-Dill, C.J. (2016). MaizeGDB update: new tools, data and interface for the
1127 maize model organism database. Nucleic acids research 44, D1195-1201.
- 1128 Bass, H.W., Webster, C., Obrian, G.R., Roberts, J.K.M., and Boston, R.S. (1992). A Maize
1129 Ribosome-Inactivating Protein Is Controlled by the Transcriptional Activator Opaque-2.
1130 The Plant cell 4, 225-234.
- 1131 Becraft, P.W. (2001). Cell fate specification in the cereal endosperm. Seminars in cell &
1132 developmental biology 12, 387-394.
- 1133 Becraft, P.W., and Gutierrez-Marcos, J. (2012). Endosperm development: dynamic processes
1134 and cellular innovations underlying sibling altruism. Wiley interdisciplinary reviews.
1135 Developmental biology 1, 579-593.

- 1136 Bernard, L., Ciceri, P., and Viotti, A. (1994). Molecular analysis of wild-type and mutant alleles
1137 at the Opaque-2 regulatory locus of maize reveals different mutations and types of O2
1138 products. *Plant molecular biology* 24, 949-959.
- 1139 Bhat, R.A., Borst, J.W., Riehl, M., and Thompson, R.D. (2004). Interaction of maize Opaque-2
1140 and the transcriptional co-activators GCN5 and ADA2, in the modulation of
1141 transcriptional activity. *Plant molecular biology* 55, 239-252.
- 1142 Bhat, R.A., Riehl, M., Santandrea, G., Velasco, R., Slocombe, S., Donn, G., Steinbiss, H.H.,
1143 Thompson, R.D., and Becker, H.A. (2003). Alteration of GCN5 levels in maize reveals
1144 dynamic responses to manipulating histone acetylation. *The Plant journal : for cell and*
1145 *molecular biology* 33, 455-469.
- 1146 Bolger, A.M., Lohse, M., and Usadel, B. (2014). Trimmomatic: a flexible trimmer for Illumina
1147 sequence data. *Bioinformatics* 30, 2114-2120.
- 1148 Burdo, B., Gray, J., Goetting-Minesky, M.P., Wittler, B., Hunt, M., Li, T., Velliquette, D.,
1149 Thomas, J., Gentzel, I., dos Santos Brito, M., Mejia-Guerra, M.K., Connolly, L.N., Qaisi,
1150 D., Li, W., Casas, M.I., Doseff, A.I., and Grotewold, E. (2014). The Maize TFome--
1151 development of a transcription factor open reading frame collection for functional
1152 genomics. *The Plant journal : for cell and molecular biology* 80, 356-366.
- 1153 Chen, J., Zeng, B., Zhang, M., Xie, S., Wang, G., Hauck, A., and Lai, J. (2014a). Dynamic
1154 transcriptome landscape of maize embryo and endosperm development. *Plant physiology*
1155 166, 252-264.
- 1156 Chen, Y., Zhou, Z., Zhao, G., Li, X., Song, L., Yan, N., Weng, J., Hao, Z., Zhang, D., Li, M.,
1157 and Zhang, S. (2014b). Transposable element rbg induces the differential expression of
1158 opaque-2 mutant gene in two maize o2 NILs derived from the same inbred line. *PloS one*
1159 9, e85159.
- 1160 Cifuentes-Rojas, C., Kannan, K., Tseng, L., and Shippen, D.E. (2011). Two RNA subunits and
1161 POT1a are components of Arabidopsis telomerase. *Proceedings of the National Academy of*
1162 *Sciences of the United States of America* 108, 73-78.
- 1163 Coleman, C.E., and Larkins, B.A. (1999). The prolamins of maize. In *Seed Proteins* (Springer),
1164 pp. 109-139.
- 1165 Cord Neto, G., Yunes, J.A., da Silva, M.J., Vettore, A.L., Arruda, P., and Leite, A. (1995). The
1166 involvement of Opaque 2 on beta-prolamin gene regulation in maize and Coix suggests a

- 1167 more general role for this transcriptional activator. Plant molecular biology 27, 1015-
1168 1029.
- 1169 de Vetten, N.C., and Ferl, R.J. (1995). Characterization of a maize G-box binding factor that is
1170 induced by hypoxia. The Plant journal : for cell and molecular biology 7, 589-601.
- 1171 Du, Z., Zhou, X., Ling, Y., Zhang, Z., and Su, Z. (2010). agriGO: a GO analysis toolkit for the
1172 agricultural community. Nucleic acids research 38, W64-70.
- 1173 Eveland, A.L., Goldshmidt, A., Pautler, M., Morohashi, K., Liseron-Monfils, C., Lewis, M.W.,
1174 Kumari, S., Hiraga, S., Yang, F., Unger-Wallace, E., Olson, A., Hake, S., Vollbrecht, E.,
1175 Grotewold, E., Ware, D., and Jackson, D. (2014). Regulatory modules controlling maize
1176 inflorescence architecture. Genome research 24, 431-443.
- 1177 FAO. (2015). FAO Statistical Pocketbook 2015.
1178 (<http://www.fao.org/documents/card/en/c/383d384a-28e6-47b3-a1a2-2496a9e017b2/>).
- 1179 Feng, J., Liu, T., Qin, B., Zhang, Y., and Liu, X.S. (2012). Identifying ChIP-seq enrichment
1180 using MACS. Nature protocols 7, 1728-1740.
- 1181 Friedman, W.E., Madrid, E.N., and Williams, J.H. (2008). Origin of the fittest and survival of the
1182 fittest: Relating female gametophyte development to endosperm genetics. Int J Plant Sci
1183 169, 79-92.
- 1184 Frizzi, A., Caldo, R.A., Morrell, J.A., Wang, M., Lutfiyya, L.L., Brown, W.E., Malvar, T.M.,
1185 and Huang, S. (2010). Compositional and transcriptional analyses of reduced zein kernels
1186 derived from the opaque2 mutation and RNAi suppression. Plant molecular biology 73,
1187 569-585.
- 1188 Gallusci, P., Varotto, S., Matsuoko, M., Maddaloni, M., and Thompson, R.D. (1996). Regulation
1189 of cytosolic pyruvate, orthophosphate dikinase expression in developing maize
1190 endosperm. Plant molecular biology 31, 45-55.
- 1191 Gehl, C., Waadt, R., Kudla, J., Mendel, R.R., and Hansch, R. (2009). New GATEWAY vectors
1192 for high throughput analyses of protein-protein interactions by bimolecular fluorescence
1193 complementation. Molecular plant 2, 1051-1058.
- 1194 Gontarek, B.C., Neelakandan, A.K., Wu, H., and Becroft, P.W. (2016). NKD Transcription
1195 Factors Are Central Regulators of Maize Endosperm Development. The Plant cell 28,
1196 2916-2936.

- 1197 Gotz, S., Garcia-Gomez, J.M., Terol, J., Williams, T.D., Nagaraj, S.H., Nueda, M.J., Robles, M.,
1198 Talon, M., Dopazo, J., and Conesa, A. (2008). High-throughput functional annotation and
1199 data mining with the Blast2GO suite. *Nucleic acids research* 36, 3420-3435.
- 1200 Gray, J., Bevan, M., Brutnell, T., Buell, C.R., Cone, K., Hake, S., Jackson, D., Kellogg, E.,
1201 Lawrence, C., McCouch, S., Mockler, T., Moose, S., Paterson, A., Peterson, T., Rokshar,
1202 D., Souza, G.M., Springer, N., Stein, N., Timmermans, M., Wang, G.L., and Grotewold,
1203 E. (2009). A recommendation for naming transcription factor proteins in the grasses.
1204 *Plant physiology* 149, 4-6.
- 1205 Hamamura, Y., Nagahara, S., and Higashiyama, T. (2012). Double fertilization on the move.
1206 *Current opinion in plant biology* 15, 70-77.
- 1207 Hartings, H., Lauria, M., Lazzaroni, N., Pirona, R., and Motto, M. (2011). The Zea mays mutants
1208 opaque-2 and opaque-7 disclose extensive changes in endosperm metabolism as revealed
1209 by protein, amino acid, and transcriptome-wide analyses. *BMC genomics* 12, 41.
- 1210 Hoecker, U., Vasil, I.K., and McCarty, D.R. (1995). Integrated control of seed maturation and
1211 germination programs by activator and repressor functions of Viviparous-1 of maize.
1212 *Genes & development* 9, 2459-2469.
- 1213 Hoecker, U., Vasil, I.K., and McCarty, D.R. (1999). Signaling from the embryo conditions Vp1-
1214 mediated repression of alpha-amylase genes in the aleurone of developing maize seeds.
1215 *The Plant journal : for cell and molecular biology* 19, 371-377.
- 1216 Holding, D.R., Hunter, B.G., Chung, T., Gibbon, B.C., Ford, C.F., Bharti, A.K., Messing, J.,
1217 Hamaker, B.R., and Larkins, B.A. (2008). Genetic analysis of opaque2 modifier loci in
1218 quality protein maize. *TAG. Theoretical and applied genetics. Theoretische und
1219 angewandte Genetik* 117, 157-170.
- 1220 Hunter, B.G., Beatty, M.K., Singletary, G.W., Hamaker, B.R., Dilkes, B.P., Larkins, B.A., and
1221 Jung, R. (2002). Maize opaque endosperm mutations create extensive changes in patterns
1222 of gene expression. *The Plant cell* 14, 2591-2612.
- 1223 Hwang, Y.S., Ciceri, P., Parsons, R.L., Moose, S.P., Schmidt, R.J., and Huang, N. (2004). The
1224 maize O2 and PBF proteins act additively to promote transcription from storage protein
1225 gene promoters in rice endosperm cells. *Plant & cell physiology* 45, 1509-1518.

- 1226 Jia, H., Nettleton, D., Peterson, J.M., Vazquez-Carrillo, G., Jannink, J.L., and Scott, M.P. (2007).
1227 Comparison of transcript profiles in wild-type and o2 maize endosperm in different
1228 genetic backgrounds. *Crop Science* 47, S45-S59.
- 1229 Jia, M., Wu, H., Clay, K.L., Jung, R., Larkins, B.A., and Gibbon, B.C. (2013). Identification and
1230 characterization of lysine-rich proteins and starch biosynthesis genes in the opaque2
1231 mutant by transcriptional and proteomic analysis. *BMC plant biology* 13, 60.
- 1232 Jin, J., Zhang, H., Kong, L., Gao, G., and Luo, J. (2014). PlantTFDB 3.0: a portal for the
1233 functional and evolutionary study of plant transcription factors. *Nucleic acids research* 42,
1234 D1182-1187.
- 1235 Kemper, E.L., Neto, G.C., Papes, F., Moraes, K.C., Leite, A., and Arruda, P. (1999). The role of
1236 opaque2 in the control of lysine-degrading activities in developing maize endosperm. *The
1237 Plant cell* 11, 1981-1994.
- 1238 Kent, W.J. (2002). BLAT--the BLAST-like alignment tool. *Genome research* 12, 656-664.
- 1239 Kodrzycki, R., Boston, R.S., and Larkins, B.A. (1989). The opaque-2 mutation of maize
1240 differentially reduces zein gene transcription. *The Plant cell* 1, 105-114.
- 1241 Kusano, T., Berberich, T., Harada, M., Suzuki, N., and Sugawara, K. (1995). A maize DNA-
1242 binding factor with a bZIP motif is induced by low temperature. *Molecular & general
1243 genetics : MGG* 248, 507-517.
- 1244 Langmead, B., and Salzberg, S.L. (2012). Fast gapped-read alignment with Bowtie 2. *Nature
1245 methods* 9, 357-359.
- 1246 Larkins, B.A., Wu, Y., Song, R., and Messing, J. (2017). Maize Seed Storage Proteins. In *Maize
1247 Kernel Development*, B.A. Larkins, ed (CAB International), pp. 175-189.
- 1248 Leroux, B.M., Goodyke, A.J., Schumacher, K.I., Abbott, C.P., Clore, A.M., Yadegari, R.,
1249 Larkins, B.A., and Dannenhoffer, J.M. (2014). Maize early endosperm growth and
1250 development: from fertilization through cell type differentiation. *American journal of
1251 botany* 101, 1259-1274.
- 1252 Li, C., Qiao, Z., Qi, W., Wang, Q., Yuan, Y., Yang, X., Tang, Y., Mei, B., Lv, Y., Zhao, H.,
1253 Xiao, H., and Song, R. (2015). Genome-wide characterization of cis-acting DNA targets
1254 reveals the transcriptional regulatory framework of opaque2 in maize. *The Plant cell* 27,
1255 532-545.

- 1256 Li, G., Wang, D., Yang, R., Logan, K., Chen, H., Zhang, S., Skaggs, M.I., Lloyd, A., Burnett,
1257 W.J., Laurie, J.D., Hunter, B.G., Dannenhoffer, J.M., Larkins, B.A., Drews, G.N., Wang,
1258 X., and Yadegari, R. (2014). Temporal patterns of gene expression in developing maize
1259 endosperm identified through transcriptome sequencing. *Proceedings of the National
1260 Academy of Sciences of the United States of America* 111, 7582-7587.
- 1261 Li, J., and Berger, F. (2012). Endosperm: food for humankind and fodder for scientific
1262 discoveries. *The New phytologist* 195, 290-305.
- 1263 Li, Q., Wang, J., Ye, J., Zheng, X., Xiang, X., Li, C., Fu, M., Wang, Q., Zhang, Z.Y., and Wu, Y.
1264 (2017). The Maize Imprinted Gene Floury3 Encodes a PLATZ Protein Required for
1265 tRNA and 5S rRNA Transcription Through Interaction with RNA Polymerase III. *The
1266 Plant cell*.
- 1267 Locatelli, S., Piatti, P., Motto, M., and Rossi, V. (2009). Chromatin and DNA modifications in
1268 the Opaque2-mediated regulation of gene transcription during maize endosperm
1269 development. *The Plant cell* 21, 1410-1427.
- 1270 Lohmer, S., Maddaloni, M., Motto, M., Di Fonzo, N., Hartings, H., Salamini, F., and Thompson,
1271 R.D. (1991). The maize regulatory locus Opaque-2 encodes a DNA-binding protein
1272 which activates the transcription of the b-32 gene. *The EMBO journal* 10, 617-624.
- 1273 Machanick, P., and Bailey, T.L. (2011). MEME-ChIP: motif analysis of large DNA datasets.
1274 *Bioinformatics* 27, 1696-1697.
- 1275 Maddaloni, M., Di Fonzo, N., Hartings, H., Lazzaroni, N., Salamini, F., Thompson, R., and
1276 Motto, M. (1989). The sequence of the zein regulatory gene opaque-2 (O2) of Zea Mays.
1277 *Nucleic acids research* 17, 7532.
- 1278 Maddaloni, M., Donini, G., Balconi, C., Rizzi, E., Gallusci, P., Forlani, F., Lohmer, S.,
1279 Thompson, R., Salamini, F., and Motto, M. (1996). The transcriptional activator Opaque-
1280 2 controls the expression of a cytosolic form of pyruvate orthophosphate dikinase-1 in
1281 maize endosperms. *Molecular & general genetics : MGG* 250, 647-654.
- 1282 Mangan, S., and Alon, U. (2003). Structure and function of the feed-forward loop network motif.
1283 *Proceedings of the National Academy of Sciences of the United States of America* 100,
1284 11980-11985.
- 1285 Mathelier, A., Zhao, X., Zhang, A.W., Parcy, F., Worsley-Hunt, R., Arenillas, D.J., Buchman, S.,
1286 Chen, C.Y., Chou, A., Ienasescu, H., Lim, J., Shyr, C., Tan, G., Zhou, M., Lenhard, B.,

- 1287 Sandelin, A., and Wasserman, W.W. (2014). JASPAR 2014: an extensively expanded
1288 and updated open-access database of transcription factor binding profiles. Nucleic acids
1289 research 42, D142-147.
- 1290 Mertz, E.T., Bates, L.S., and Nelson, O.E. (1964). Mutant gene that changes protein composition
1291 and increases lysine content of maize endosperm. Science 145, 279-280.
- 1292 Morohashi, K., Casas, M.I., Falcone Ferreyra, M.L., Mejia-Guerra, M.K., Pourcel, L., Yilmaz,
1293 A., Feller, A., Carvalho, B., Emiliani, J., Rodriguez, E., Pellegrinet, S., McMullen, M.,
1294 Casati, P., and Grotewold, E. (2012). A genome-wide regulatory framework identifies
1295 maize pericarp color1 controlled genes. The Plant cell 24, 2745-2764.
- 1296 Muth, J.R., Muller, M., Lohmer, S., Salamini, F., and Thompson, R.D. (1996). The role of
1297 multiple binding sites in the activation of zein gene expression by Opaque-2. Molecular
1298 & general genetics : MGG 252, 723-732.
- 1299 Olsen, O.A. (2001). ENDOSPERM DEVELOPMENT: Cellularization and Cell Fate
1300 Specification. Annual review of plant physiology and plant molecular biology 52, 233-
1301 267.
- 1302 Olsen, O.A. (2004). Nuclear endosperm development in cereals and *Arabidopsis thaliana*. The
1303 Plant cell 16 Suppl, S214-227.
- 1304 Pysh, L.D., and Schmidt, R.J. (1996). Characterization of the maize OHP1 gene: evidence of
1305 gene copy variability among inbreds. Gene 177, 203-208.
- 1306 Pysh, L.D., Aukerman, M.J., and Schmidt, R.J. (1993). OHP1: a maize basic domain/leucine
1307 zipper protein that interacts with opaque2. The Plant cell 5, 227-236.
- 1308 Qiao, Z., Qi, W., Wang, Q., Feng, Y., Yang, Q., Zhang, N., Wang, S., Tang, Y., and Song, R.
1309 (2016). ZmMADS47 Regulates Zein Gene Transcription through Interaction with
1310 Opaque2. PLoS genetics 12, e1005991.
- 1311 Quinlan, A.R., and Hall, I.M. (2010). BEDTools: a flexible suite of utilities for comparing
1312 genomic features. Bioinformatics 26, 841-842.
- 1313 Robinson, M.D., McCarthy, D.J., and Smyth, G.K. (2010). edgeR: a Bioconductor package for
1314 differential expression analysis of digital gene expression data. Bioinformatics 26, 139-
1315 140.
- 1316 Sabelli, P.A., and Larkins, B.A. (2009). The development of endosperm in grasses. Plant
1317 physiology 149, 14-26.

- 1318 Saleh, A., Alvarez-Venegas, R., and Avramova, Z. (2008). An efficient chromatin
1319 immunoprecipitation (ChIP) protocol for studying histone modifications in Arabidopsis
1320 plants. *Nature protocols* 3, 1018-1025.
- 1321 Schmidt, R.J., Burr, F.A., and Burr, B. (1987). Transposon tagging and molecular analysis of the
1322 maize regulatory locus opaque-2. *Science* 238, 960-963.
- 1323 Schmidt, R.J., Burr, F.A., Aukerman, M.J., and Burr, B. (1990). Maize regulatory gene opaque-2
1324 encodes a protein with a "leucine-zipper" motif that binds to zein DNA. *Proceedings of
1325 the National Academy of Sciences of the United States of America* 87, 46-50.
- 1326 Schmidt, R.J., Ketudat, M., Aukerman, M.J., and Hoschek, G. (1992). Opaque-2 is a
1327 transcriptional activator that recognizes a specific target site in 22-kD zein genes. *The
1328 Plant cell* 4, 689-700.
- 1329 Sievers, F., Wilm, A., Dineen, D., Gibson, T.J., Karplus, K., Li, W.Z., Lopez, R., McWilliam, H.,
1330 Remmert, M., Soding, J., Thompson, J.D., and Higgins, D.G. (2011). Fast, scalable
1331 generation of high-quality protein multiple sequence alignments using Clustal Omega.
1332 *Mol Syst Biol* 7.
- 1333 Stamatakis, A. (2014). RAxML version 8: a tool for phylogenetic analysis and post-analysis of
1334 large phylogenies. *Bioinformatics* 30, 1312-1313.
- 1335 Taylor-Teeple, M., Lin, L., de Lucas, M., Turco, G., Toal, T.W., Gaudinier, A., Young, N.F.,
1336 Trabucco, G.M., Veling, M.T., Lamothe, R., Handakumbura, P.P., Xiong, G., Wang, C.,
1337 Corwin, J., Tsoukalas, A., Zhang, L., Ware, D., Pauly, M., Kliebenstein, D.J., Dehesh, K.,
1338 Tagkopoulos, I., Breton, G., Pruneda-Paz, J.L., Ahnert, S.E., Kay, S.A., Hazen, S.P., and
1339 Brady, S.M. (2015). An Arabidopsis gene regulatory network for secondary cell wall
1340 synthesis. *Nature* 517, 571-575.
- 1341 Thorvaldsdottir, H., Robinson, J.T., and Mesirov, J.P. (2013). Integrative Genomics Viewer
1342 (IGV): high-performance genomics data visualization and exploration. *Briefings in
1343 bioinformatics* 14, 178-192.
- 1344 Trapnell, C., Pachter, L., and Salzberg, S.L. (2009). TopHat: discovering splice junctions with
1345 RNA-Seq. *Bioinformatics* 25, 1105-1111.
- 1346 Unger, E., Parsons, R.L., Schmidt, R.J., Bowen, B., and Roth, B.A. (1993). Dominant Negative
1347 Mutants of Opaque2 Suppress Transactivation of a 22-kD Zein Promoter by Opaque2 in
1348 Maize Endosperm Cells. *The Plant cell* 5, 831-841.

- 1349 Vicente-Carbajosa, J., Moose, S.P., Parsons, R.L., and Schmidt, R.J. (1997). A maize zinc-finger
1350 protein binds the prolamin box in zein gene promoters and interacts with the basic leucine
1351 zipper transcriptional activator Opaque2. *Proceedings of the National Academy of*
1352 *Sciences of the United States of America* 94, 7685-7690.
- 1353 Walley, J.W., Shen, Z., Sartor, R., Wu, K.J., Osborn, J., Smith, L.G., and Briggs, S.P. (2013).
1354 Reconstruction of protein networks from an atlas of maize seed proteotypes. *Proceedings*
1355 *of the National Academy of Sciences of the United States of America* 110, E4808-4817.
- 1356 Walsh, J.R., Schaeffer, M.L., Zhang, P., Rhee, S.Y., Dickerson, J.A., and Sen, T.Z. (2016). The
1357 quality of metabolic pathway resources depends on initial enzymatic function
1358 assignments: a case for maize. *BMC systems biology* 10, 129.
- 1359 Wang, D., Tyson, M.D., Jackson, S.S., and Yadegari, R. (2006). Partially redundant functions of
1360 two SET-domain polycomb-group proteins in controlling initiation of seed development
1361 in Arabidopsis. *Proceedings of the National Academy of Sciences of the United States of*
1362 *America* 103, 13244-13249.
- 1363 Wang, D., Zhang, C., Hearn, D.J., Kang, I.H., Punwani, J.A., Skaggs, M.I., Drews, G.N.,
1364 Schumaker, K.S., and Yadegari, R. (2010). Identification of transcription-factor genes
1365 expressed in the Arabidopsis female gametophyte. *BMC plant biology* 10, 110.
- 1366 Whelan, S., and Goldman, N. (2001). A general empirical model of protein evolution derived
1367 from multiple protein families using a maximum-likelihood approach. *Molecular biology*
1368 *and evolution* 18, 691-699.
- 1369 Woo, Y.M., Hu, D.W., Larkins, B.A., and Jung, R. (2001). Genomics analysis of genes
1370 expressed in maize endosperm identifies novel seed proteins and clarifies patterns of zein
1371 gene expression. *The Plant cell* 13, 2297-2317.
- 1372 Wu, Y., and Messing, J. (2012). Rapid divergence of prolamin gene promoters of maize after
1373 gene amplification and dispersal. *Genetics* 192, 507-519.
- 1374 Wu, Y., and Messing, J. (2014). Proteome balancing of the maize seed for higher nutritional
1375 value. *Frontiers in plant science* 5, 240.
- 1376 Xu, J.H., and Messing, J. (2008). Diverged copies of the seed regulatory Opaque-2 gene by a
1377 segmental duplication in the progenitor genome of rice, sorghum, and maize. *Molecular*
1378 *plant* 1, 760-769.

- 1379 Yan, D., Duermeyer, L., Leoveanu, C., and Nambara, E. (2014). The Functions of the
1380 Endosperm During Seed Germination. *Plant & cell physiology* 55, 1521-1533.
- 1381 Yang, J., Ji, C., and Wu, Y. (2016). Divergent Transactivation of Maize Storage Protein Zein
1382 Genes by the Transcription Factors Opaque2 and OHPs. *Genetics* 204, 581-591.
- 1383 Yi, G., Neelakandan, A.K., Gontarek, B.C., Vollbrecht, E., and Becraft, P.W. (2015). The naked
1384 endosperm genes encode duplicate INDETERMINATE domain transcription factors
1385 required for maize endosperm cell patterning and differentiation. *Plant physiology* 167,
1386 443-456.
- 1387 Yilmaz, A., Nishiyama, M.Y., Jr., Fuentes, B.G., Souza, G.M., Janies, D., Gray, J., and
1388 Grotewold, E. (2009). GRASSIUS: a platform for comparative regulatory genomics
1389 across the grasses. *Plant physiology* 149, 171-180.
- 1390 Zhan, J., Dannenhoffer, J.M., and Yadegari, R. (2017). Endosperm Development and Cell
1391 Specialization. In *Maize Kernel Development*, B.A. Larkins, ed (CAB International), pp.
1392 28-43.
- 1393 Zhan, J., Thakare, D., Ma, C., Lloyd, A., Nixon, N.M., Arakaki, A.M., Burnett, W.J., Logan,
1394 K.O., Wang, D., Wang, X., Drews, G.N., and Yadegari, R. (2015). RNA sequencing of
1395 laser-capture microdissected compartments of the maize kernel identifies regulatory
1396 modules associated with endosperm cell differentiation. *The Plant cell* 27, 513-531.
- 1397 Zhang, Y., Liu, T., Meyer, C.A., Eeckhoute, J., Johnson, D.S., Bernstein, B.E., Nusbaum, C.,
1398 Myers, R.M., Brown, M., Li, W., and Liu, X.S. (2008). Model-based analysis of ChIP-
1399 Seq (MACS). *Genome biology* 9, R137.
- 1400 Zhang, Z., Yang, J., and Wu, Y. (2015). Transcriptional Regulation of Zein Gene Expression in
1401 Maize through the Additive and Synergistic Action of opaque2, Prolamine-Box Binding
1402 Factor, and O2 Heterodimerizing Proteins. *The Plant cell* 27, 1162-1172.
- 1403 Zhang, Z., Zheng, X., Yang, J., Messing, J., and Wu, Y. (2016). Maize endosperm-specific
1404 transcription factors O2 and PBF network the regulation of protein and starch synthesis.
1405 Proceedings of the National Academy of Sciences of the United States of America 113,
1406 10842-10847.
- 1407
- 1408 FIGURE LEGENDS

1409 **Figure 1.** Identification of direct and indirect O₂ target genes using RNA-Seq and ChIP-Seq. (A)
1410 Scatter plot of log₂FC versus log₂RPKM (average in all 6 RNA-Seq samples) of all the genes
1411 tested for differential expression. DEGs are represented by red dots, and the other genes blue.
1412 Dashed lines indicate 2-fold changes (log₂FC = ±1). (B) Distribution of O₂ peaks in the maize
1413 genome based on localization of peak summits. (C) Venn diagram of numbers of O₂-modulated
1414 genes and O₂-bound genes detected by RNA-Seq and ChIP-Seq. (D) Expression levels of the
1415 O₂-modulated and/or bound gene sets in WT versus *o2* mutant. Colored boxes represent the
1416 interquartile range, horizontal lines within the boxes the median, whiskers 1.5 times the
1417 interquartile range, and black dots the outliers. (E) Distribution of O₂ peaks around the gene
1418 models of direct O₂ targets. The 5 kb genomic regions up- or downstream gene models were
1419 divided into 50 bins, while the representative gene model showing the average length of maize
1420 genes (about 2.2 kb based on the B73 gene model annotation) were divided into 22 bins. (F) Two
1421 bZIP-like motifs and their positional distributions around the summits of peaks associated with
1422 direct O₂ targets. The *P* values were calculated using the CentriMo program.

1423 **Figure 2.** Associated biological functions of O₂-regulated genes based on GO term enrichments
1424 of the O₂-modulated and/or bound gene sets. Treemap representations of GO term enrichments
1425 for the O₂-activated direct target (A), O₂-activated indirect target (B) and O₂-repressed indirect
1426 target (C) gene sets. GO terms are grouped based on the main categories, including molecular
1427 function, biological process, and cellular component. Size and color of the squares/rectangles
1428 indicates significance of enrichment (-log₁₀FDR). Abbreviations: BP, biological process; CC,
1429 cellular component; MF, molecular function.

1430 **Figure 3.** Analysis of zein genes regulated by O₂. Gene numbers and log₂FC (mean ± SEM) of
1431 zein gene families/sub-families modulated and/or bound by O₂.

1432 **Figure 4.** Temporal expression patterns of O₂-modulated and/or bound genes during endosperm
1433 development. (A) Relationships of the O₂-modulated and/or bound gene sets with the previously
1434 published temporally upregulated gene sets (Li et al., 2014). The heat map indicates *P* values (-
1435 log₁₀) of hypergeometric tests of overrepresentation of genes in a given pair of gene sets. Boxes
1436 contain the numbers of overlapping genes and the associated *P* values (in parentheses). The O₂-
1437 modulated and/or bound gene sets are noted on the *x* axis and the temporal gene sets are noted on
1438 the *y* axis. Numbers of genes in each temporal gene set: up@2DAP, 54; up@3DAP, 68;

1439 up@4DAP, 92; up@6DAP, 523; up@8DAP, 1,402; up@10DAP, 552; up@12DAP, 241. (B)
1440 through (M) The mRNA levels of 12 O2-activated direct targets in the developing endosperm of
1441 WT versus *o2* quantified using RT-qPCR. As a canonical non-zein target of O2, the *b-32* gene,
1442 although not detected as an O2-bound gene in our ChIP-Seq analysis, was also included. Data
1443 are normalized Ct values (mean \pm SEM; $n = 3$). Asterisks indicate significant difference between
1444 WT and *o2* ($|\Delta\Delta Ct| > 1$; $P < 0.05$, Student's *t* test). Blue dashed lines indicate undetectable
1445 mRNA level (Ct = 36).

1446 **Figure 5.** Expression patterns of the TF genes directly regulated by O2 during maize
1447 development. The selected expression data, based on the available maize expression atlas (Chen
1448 et al., 2014a), include vegetative (Veg) tissues shoots (Sh), roots (R), Leaf (L), shoot apical
1449 meristem (SAM, replicate 1); reproductive (Rep) tissues ear (E), tassel (T, replicate 1), pre-
1450 emergence cob (C), silk (Si), Anther (A), ovule (O), pollen (P); and whole kernels, endosperm,
1451 and embryos of different developmental stages (in DAP).

1452 **Figure 6.** O2 and bZIP17 proteins interact and co-activate target gene expression. (A) O2
1453 interacts with bZIP17 *in planta*. Fluorescent and corresponding bright field images from the
1454 BiFC assay of interaction between O2-Venus^N and bZIP17-Venus^C. O2-Venus^N/O2-Venus^C was
1455 used as a positive control. O2LA-Venus^N/O2-Venus^C, O2LA-Venus^N/bZIP17-Venus^C, and
1456 O2LA-Venus^N/O2LA-Venus^C were used as negative controls. Bars = 40 μ m. Each assay was
1457 repeated at least 4 times. (B) Co-activation of reporter gene (*LUC*) by O2 and bZIP17 through
1458 binding to O2 peak associated with *FL2*. Data are fold inductions (mean \pm SEM; $n = 5$).
1459 Different letter indicates $P < 0.05$, one-way ANOVA with post-hoc Tukey's HSD test.

1460 **Figure 7.** O2 and NKD2 co-regulate a downstream gene network. (A) Venn diagram of numbers
1461 of putative direct targets of O2 and NKD2. (B) Co-activation of reporter gene (*LUC*) by O2 and
1462 NKD2 through binding to O2 peaks associated with *FL2*, *bZIP17*, and *TAR3*. Data are fold
1463 inductions (mean \pm SEM; $n = 5$). Different letter indicates $P < 0.05$, one-way ANOVA with post-
1464 hoc Tukey's HSD test. (C) Venn diagram of numbers of putative indirect O2 targets and direct
1465 NKD2 targets. (D) Expression patterns of *O2*, *bZIP17*, *NKD1*, *NKD2*, and *VP1* in 8-DAP kernel
1466 compartments based on RNA-Seq data from Zhan et al. (2015). The heat map was hierarchically
1467 clustered on Euclidean distance. (E) Relationships of the O2-modulated and/or bound gene sets
1468 with the previously published endosperm cell-type-specifically expressed gene sets (Zhan et al.,

1469 2015). The heat map indicates *P* values ($-\log_{10}$) of hypergeometric tests of overrepresentation of
1470 genes in a given pair of gene sets. Boxes contain the numbers of overlapping genes and the
1471 associated *P* values (in parentheses). The heat map was hierarchically clustered on Euclidean
1472 distance. The O2-modulated and/or bound gene sets are noted on the *x* axis and the 8-DAP
1473 compartment-specific gene sets are noted on the *y* axis. Numbers of genes in each gene set are
1474 indicated in parentheses.

1475 **Figure 8.** Model for co-regulation of maize seed development and germination by O2, bZIP17,
1476 and NKD2. With direct mutual regulation and/or protein-protein interactions with bZIP17 or
1477 NKD2, O2 directly regulates genes involved in aleurone versus starchy endosperm
1478 differentiation, storage-protein synthesis, and abiotic stress responses of the endosperm; O2
1479 indirectly regulates genes involved synthesis/metabolism of storage proteins, carbohydrates, and
1480 lipids; and O2 indirectly regulates *VP1*, which in turn regulates seed maturation and germination.

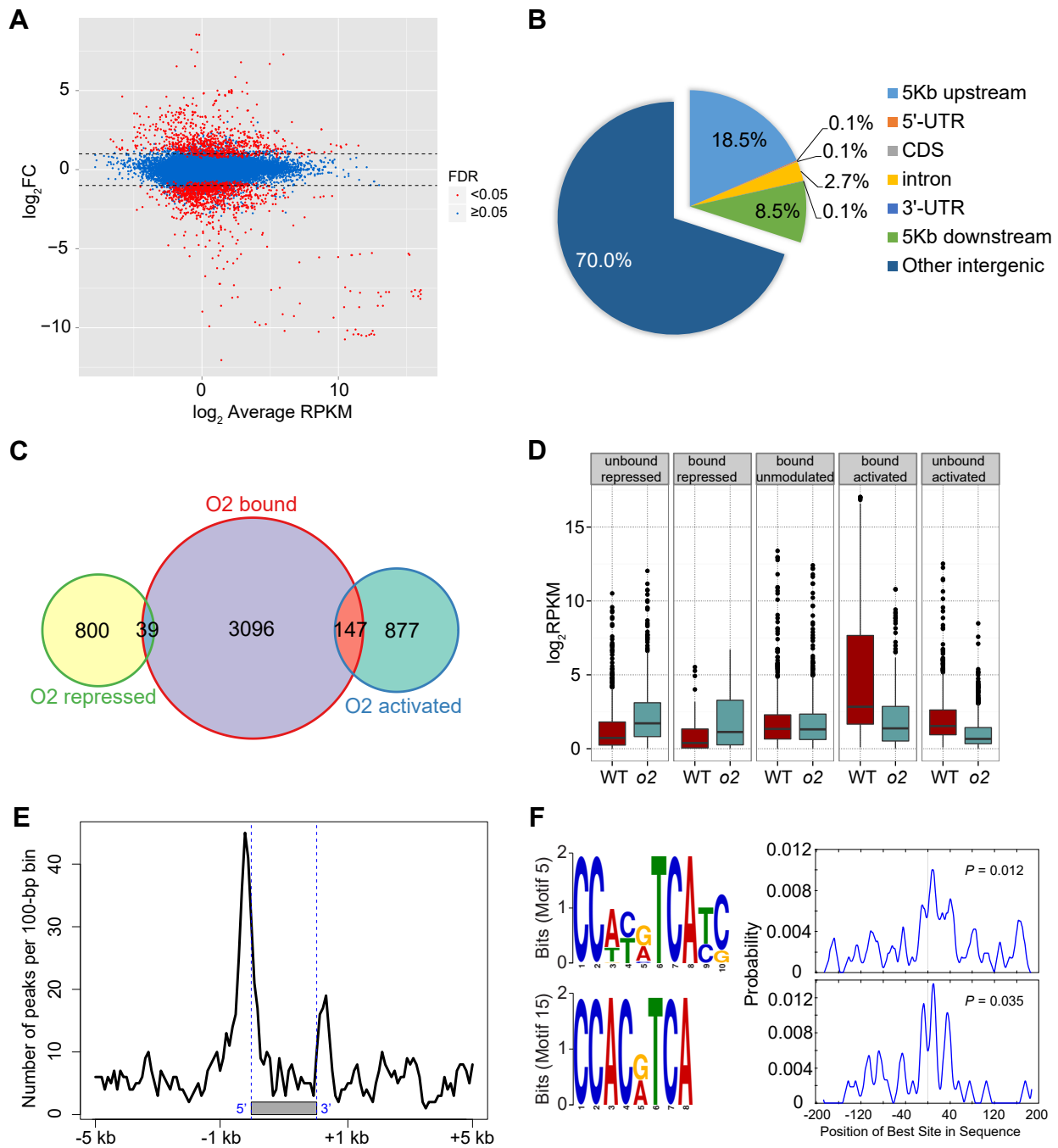


Figure 1. Identification of direct and indirect O2 target genes using RNA-Seq and ChIP-Seq. (A) Scatter plot of $\log_2\text{FC}$ versus $\log_2\text{RPKM}$ (average in all 6 RNA-Seq samples) of all the genes tested for differential expression. DEGs are represented by red dots, and the other genes blue. Dashed lines indicate 2-fold changes ($\log_2\text{FC} = \pm 1$). (B) Distribution of O2 peaks in the maize genome based on localization of peak summits. (C) Venn diagram of numbers of O2-modulated genes and O2-bound genes detected by RNA-Seq and ChIP-Seq. (D) Expression levels of the O2-modulated and/or bound gene sets in WT versus *o2* mutant. Colored boxes represent the interquartile range, horizontal lines within the boxes the median, whiskers 1.5 times the interquartile range, and black dots the outliers. (E) Distribution of O2 peaks around the gene models of direct O2 targets. The 5 kb genomic regions up- or downstream gene models were divided into 50 bins, while the representative gene model showing the average length of maize genes (about 2.2 kb based on the B73 gene model annotation) were divided into 22 bins. (F) Two bZIP-like motifs and their positional distributions around the summits of peaks associated with direct O2 targets. The *P* values were calculated using the CentriMo program.

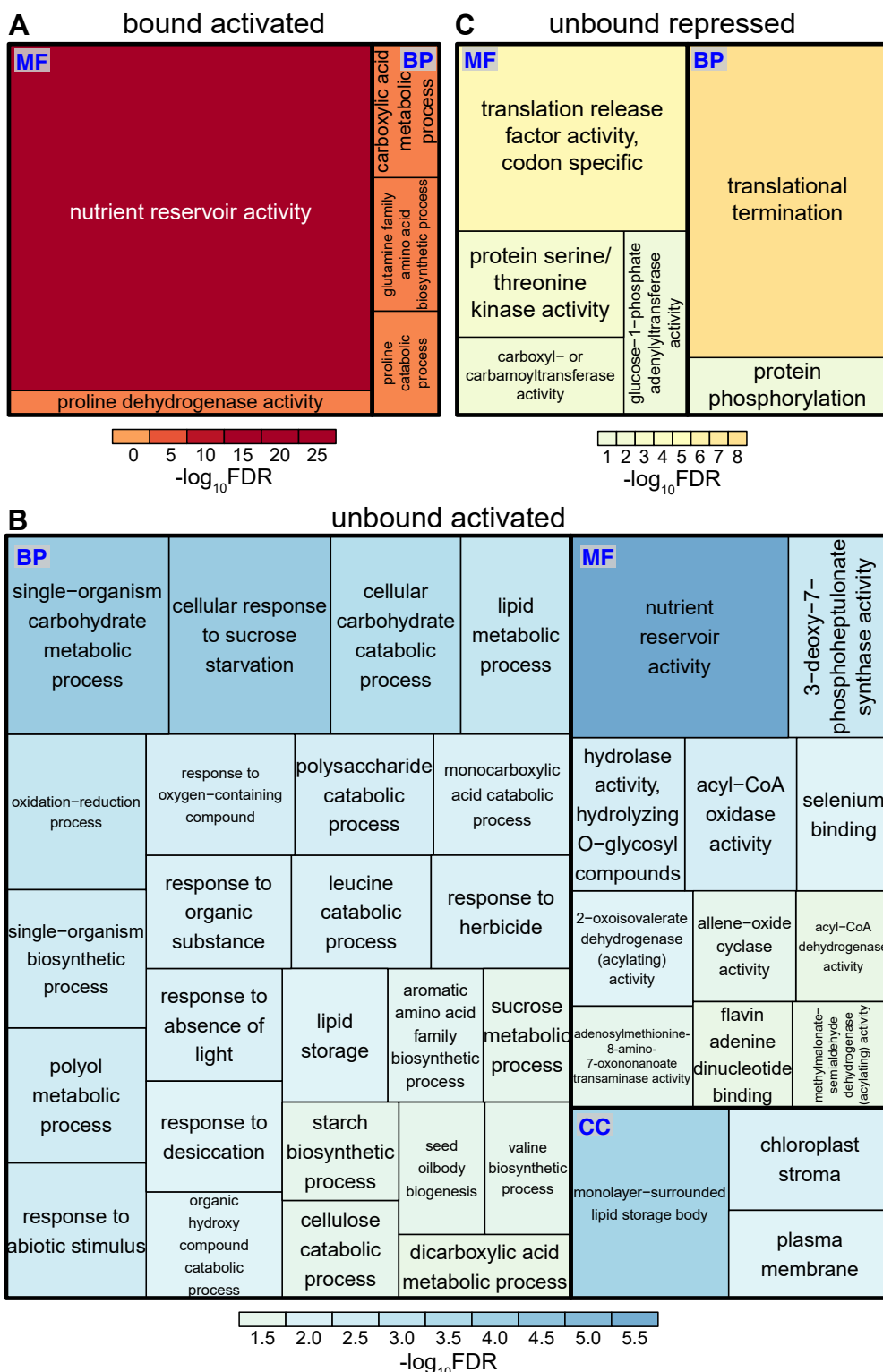


Figure 2. Associated biological functions of O₂-regulated genes based on GO term enrichments of the O₂-modulated and/or bound gene sets. Treemap representations of GO term enrichments for the O₂-activated direct target (A), O₂-activated indirect target (B) and O₂-repressed indirect target (C) gene sets. GO terms are grouped based on the main categories, including molecular function, biological process, and cellular component. Size and color of the squares/rectangles indicates significance of enrichment (-log₁₀FDR). Abbreviations: BP, biological process; CC, cellular component; MF, molecular

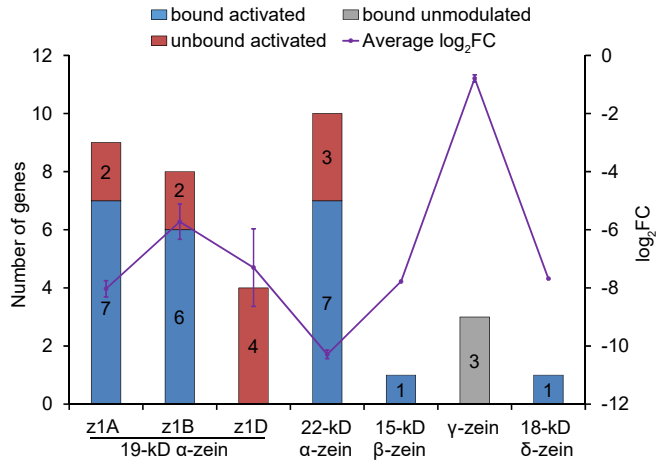


Figure 3. Analysis of zein genes regulated by O2. Gene numbers and \log_2 FC (mean \pm SEM) of zein gene families/sub-families modulated and/or bound by O2.

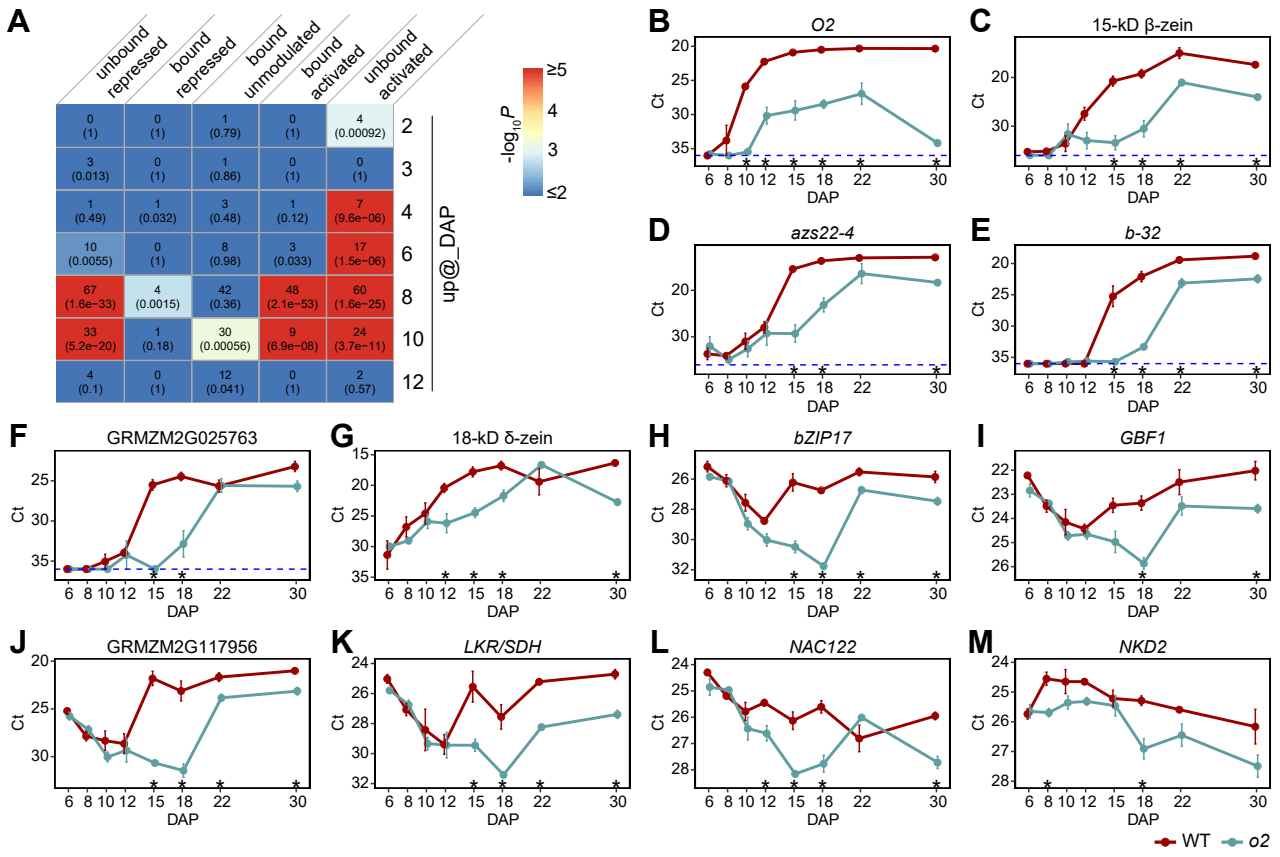


Figure 4. Temporal expression patterns of O2-modulated and/or bound genes during endosperm development. (A) Relationships of the O2-modulated and/or bound gene sets with the previously published temporally upregulated gene sets (Li et al., 2014). The heat map indicates P values ($-\log_{10}$) of hypergeometric tests of overrepresentation of genes in a given pair of gene sets. Boxes contain the numbers of overlapping genes and the associated P values (in parentheses). The O2-modulated and/or bound gene sets are noted on the x axis and the temporal gene sets are noted on the y axis. Numbers of genes in each temporal gene set: up@2DAP, 54; up@3DAP, 68; up@4DAP, 92; up@6DAP, 523; up@8DAP, 1,402; up@10DAP, 552; up@12DAP, 241. (B) through (M) The mRNA levels of 12 O2-activated direct targets in the developing endosperm of WT versus *o2* quantified using RT-qPCR. As a canonical non-zein target of O2, the *b-32* gene, although not detected as an O2-bound gene in our ChIP-Seq analysis, was also included. Data are normalized Ct values (mean \pm SEM; $n = 3$). Asterisks indicate significant difference between WT and *o2* ($|\Delta \text{Ct}| > 1$; $P < 0.05$, Student's *t* test). Blue dashed lines indicate undetectable mRNA level ($\text{Ct} = 36$).

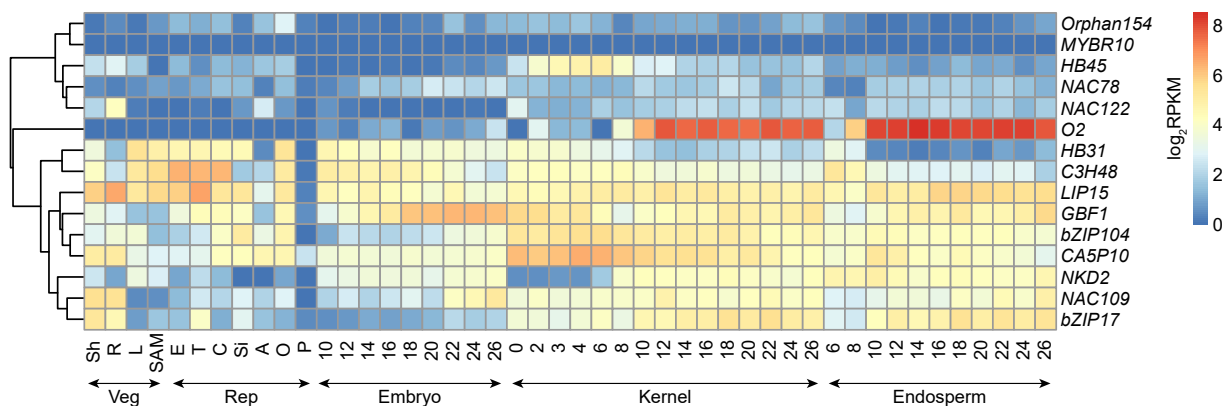


Figure 5. Expression patterns of the TF genes directly regulated by O2 during maize development. The selected expression data, based on the available maize expression atlas (Chen et al., 2014a), include vegetative (Veg) tissues shoots (Sh), roots (R), Leaf (L), shoot apical meristem (SAM, replicate 1); reproductive (Rep) tissues ear (E), tassel (T, replicate 1), pre-emergence cob (C), silk (Si), Anther (A), ovule (O), pollen (P); and whole kernels, endosperm, and embryos of different developmental stages (in DAP).

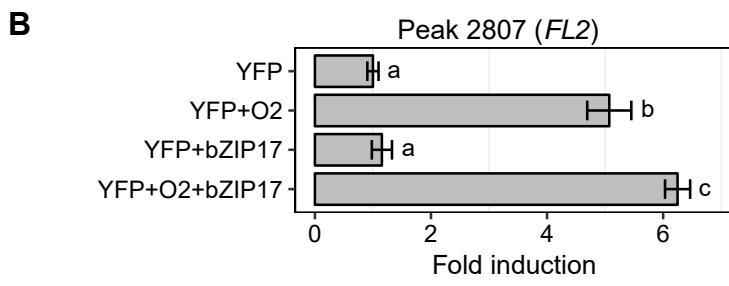
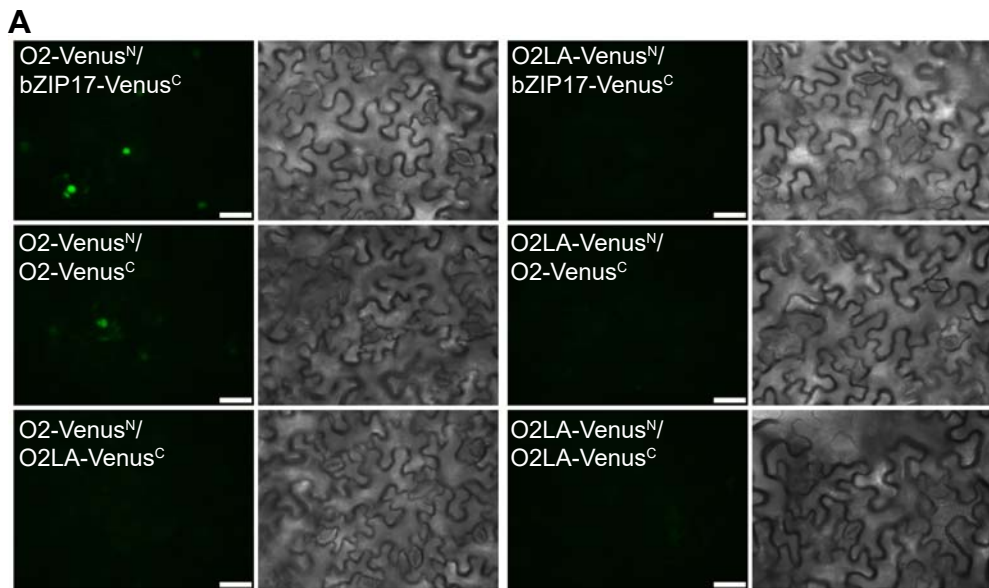


Figure 6. O2 and bZIP17 proteins interact and co-activate target gene expression. (A) O2 interacts with bZIP17 *in planta*. Fluorescent and corresponding bright field images from the BiFC assay of interaction between O2-Venus^N and bZIP17-Venus^C. O2-Venus^N/O2-Venus^C was used as a positive control. O2LA-Venus^N/O2-Venus^C, O2LA-Venus^N/bZIP17-Venus^C, and O2LA-Venus^N/O2LA-Venus^C were used as negative controls. Bars = 40 µm. Each assay was repeated at least 4 times. (B) Co-activation of reporter gene (*LUC*) by O2 and bZIP17 through binding to O2 peak associated with *FL2*. Data are fold inductions (mean ± SEM; *n* = 5). Different letter indicates *P* < 0.05, one-way ANOVA with post-hoc Tukey's HSD test.

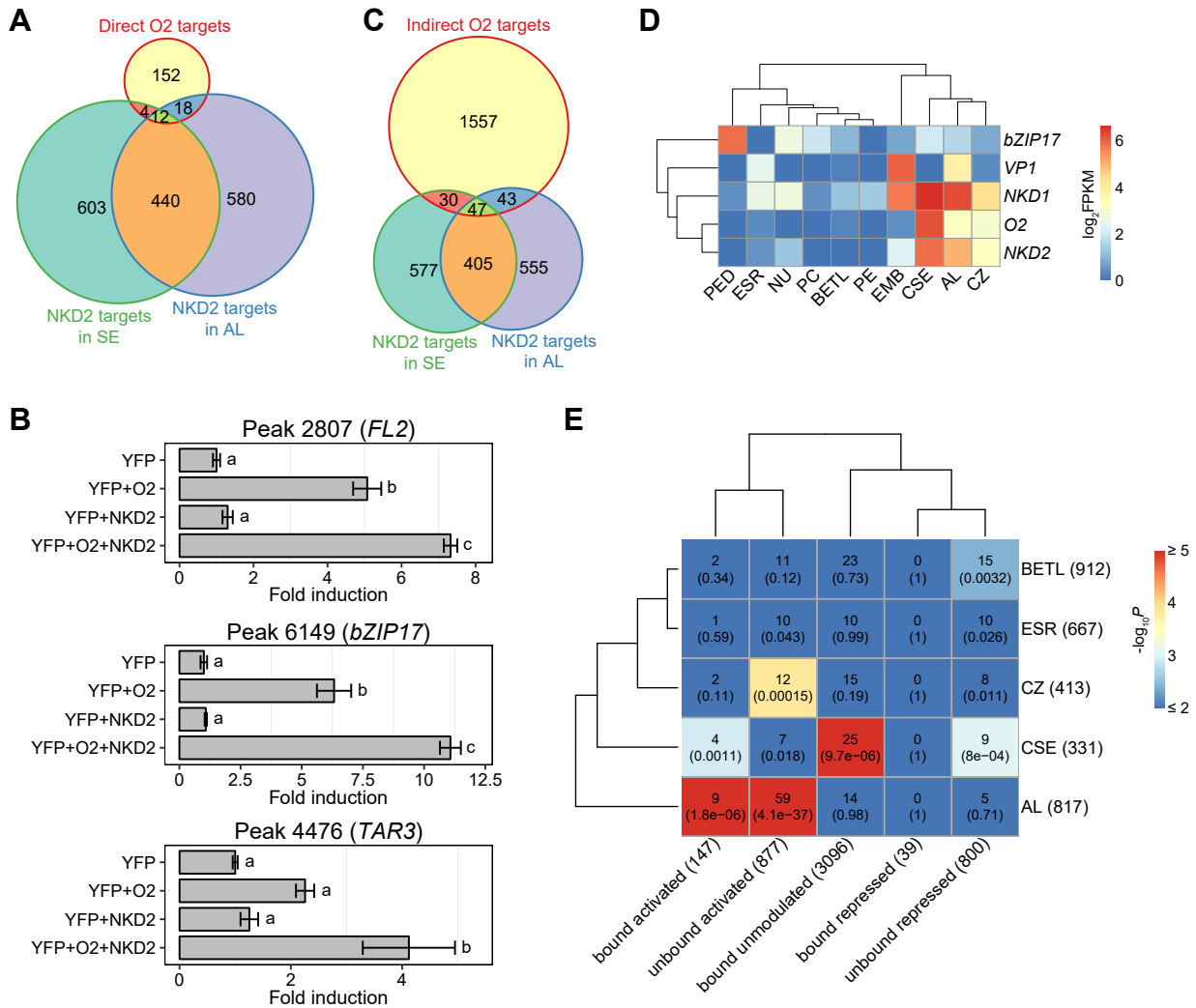


Figure 7. O₂ and NKD2 co-regulate a downstream gene network. (A) Venn diagram of numbers of putative direct targets of O₂ and NKD2. (B) Co-activation of reporter gene (*LUC*) by O₂ and NKD2 through binding to O₂ peaks associated with *FL2*, *bZIP17*, and *TAR3*. Data are fold inductions (mean \pm SEM; $n = 5$). Different letter indicates $P < 0.05$, one-way ANOVA with post-hoc Tukey's HSD test. (C) Venn diagram of numbers of putative indirect O₂ targets and direct NKD2 targets. (D) Expression patterns of O₂, *bZIP17*, *NKD1*, *NKD2*, and *VP1* in 8-DAP kernel compartments based on RNA-Seq data from Zhan et al. (2015). The heat map was hierarchically clustered on Euclidean distance. (E) Relationships of the O₂-modulated and/or bound gene sets with the previously published endosperm cell-type-specifically expressed gene sets (Zhan et al., 2015). The heat map indicates P values ($-\log_{10}$) of hypergeometric tests of overrepresentation of genes in a given pair of gene sets. Boxes contain the numbers of overlapping genes and the associated P values (in parentheses). The heat map was hierarchically clustered on Euclidean distance. The O₂-modulated and/or bound gene sets are noted on the x axis and the 8-DAP compartment-specific gene sets are noted on the y axis. Numbers of genes in each gene set are indicated in parentheses.

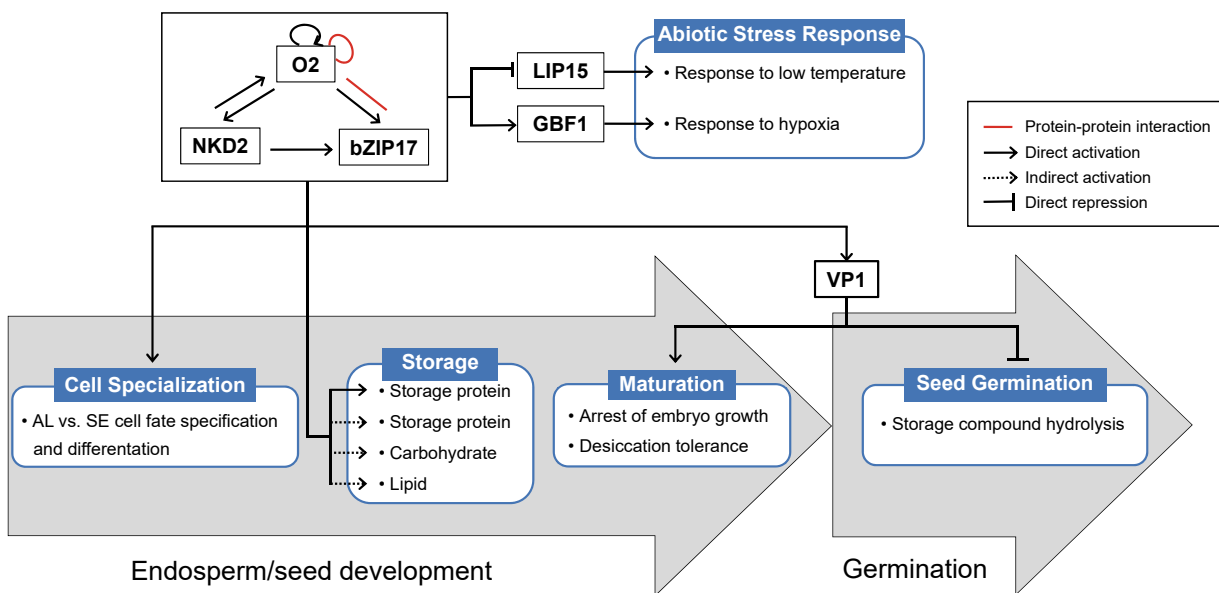


Figure 8. Model for co-regulation of maize seed development and germination by O2, bZIP17, and NKD2. With direct mutual regulation and/or protein-protein interactions with bZIP17 or NKD2, O2 directly regulates genes involved in aleurone versus starchy endosperm differentiation, storage-protein synthesis, and abiotic stress responses of the endosperm; O2 indirectly regulates genes involved in synthesis/metabolism of storage proteins, carbohydrates, and lipids; and O2 indirectly regulates VP1, which in turn regulates seed maturation and germination.

Parsed Citations

Andorf, C.M., Cannon, E.K., Portwood, J.L., 2nd, Gardiner, J.M., Harper, L.C., Schaeffer, M.L., Braun, B.L., Campbell, D.A., Vinnakota, A.G., Sribalusu, V.V., Huerta, M., Cho, K.T., Wimalanathan, K., Richter, J.D., Mauch, E.D., Rao, B.S., Birkett, S.M., Sen, T.Z., and Lawrence-Dill, C.J. (2016). MaizeGDB update: new tools, data and interface for the maize model organism database. *Nucleic acids research* 44, D1195-1201.

Pubmed: [Author and Title](#)

Google Scholar: [Author Only Title Only Author and Title](#)

Bass, H.W., Webster, C., Obrian, G.R., Roberts, J.K.M., and Boston, R.S. (1992). A Maize Ribosome-Inactivating Protein Is Controlled by the Transcriptional Activator Opaque-2. *The Plant cell* 4, 225-234.

Pubmed: [Author and Title](#)

Google Scholar: [Author Only Title Only Author and Title](#)

Becraft, P.W. (2001). Cell fate specification in the cereal endosperm. *Seminars in cell & developmental biology* 12, 387-394.

Pubmed: [Author and Title](#)

Google Scholar: [Author Only Title Only Author and Title](#)

Becraft, P.W., and Gutierrez-Marcos, J. (2012). Endosperm development: dynamic processes and cellular innovations underlying sibling altruism. *Wiley interdisciplinary reviews. Developmental biology* 1, 579-593.

Pubmed: [Author and Title](#)

Google Scholar: [Author Only Title Only Author and Title](#)

Bernard, L., Ciceri, P., and Viotti, A (1994). Molecular analysis of wild-type and mutant alleles at the Opaque-2 regulatory locus of maize reveals different mutations and types of O2 products. *Plant molecular biology* 24, 949-959.

Pubmed: [Author and Title](#)

Google Scholar: [Author Only Title Only Author and Title](#)

Bhat, R.A., Borst, J.W., Riehl, M., and Thompson, R.D. (2004). Interaction of maize Opaque-2 and the transcriptional co-activators GCN5 and ADA2, in the modulation of transcriptional activity. *Plant molecular biology* 55, 239-252.

Pubmed: [Author and Title](#)

Google Scholar: [Author Only Title Only Author and Title](#)

Bhat, R.A., Riehl, M., Santandrea, G., Velasco, R., Slocombe, S., Donn, G., Steinbiss, H.H., Thompson, R.D., and Becker, H.A. (2003). Alteration of GCN5 levels in maize reveals dynamic responses to manipulating histone acetylation. *The Plant journal : for cell and molecular biology* 33, 455-469.

Pubmed: [Author and Title](#)

Google Scholar: [Author Only Title Only Author and Title](#)

Bolger, A.M., Lohse, M., and Usadel, B. (2014). Trimmomatic: a flexible trimmer for Illumina sequence data. *Bioinformatics* 30, 2114-2120.

Pubmed: [Author and Title](#)

Google Scholar: [Author Only Title Only Author and Title](#)

Burdo, B., Gray, J., Goetting-Minesky, M.P., Wittler, B., Hunt, M., Li, T., Velliquette, D., Thomas, J., Gentzel, I., dos Santos Brito, M., Mejia-Guerra, M.K., Connolly, L.N., Qaisi, D., Li, W., Casas, M.I., Doseff, A.I., and Grotewold, E. (2014). The Maize TFome--development of a transcription factor open reading frame collection for functional genomics. *The Plant journal : for cell and molecular biology* 80, 356-366.

Pubmed: [Author and Title](#)

Google Scholar: [Author Only Title Only Author and Title](#)

Chen, J., Zeng, B., Zhang, M., Xie, S., Wang, G., Hauck, A., and Lai, J. (2014a). Dynamic transcriptome landscape of maize embryo and endosperm development. *Plant physiology* 166, 252-264.

Pubmed: [Author and Title](#)

Google Scholar: [Author Only Title Only Author and Title](#)

Chen, Y., Zhou, Z., Zhao, G., Li, X., Song, L., Yan, N., Weng, J., Hao, Z., Zhang, D., Li, M., and Zhang, S. (2014b). Transposable element rbg induces the differential expression of opaque-2 mutant gene in two maize o2 NILs derived from the same inbred line. *PLoS one* 9, e85159.

Pubmed: [Author and Title](#)

Google Scholar: [Author Only Title Only Author and Title](#)

Cifuentes-Rojas, C., Kannan, K., Tseng, L., and Shippen, D.E. (2011). Two RNA subunits and POT1a are components of Arabidopsis telomerase. *Proceedings of the National Academy of Sciences of the United States of America* 108, 73-78.

Pubmed: [Author and Title](#)

Google Scholar: [Author Only Title Only Author and Title](#)

Coleman, C.E., and Larkins, B.A (1999). The prolamins of maize. In *Seed Proteins* (Springer), pp. 109-139.

Pubmed: [Author and Title](#)

Google Scholar: [Author Only Title Only Author and Title](#)

Cord Neto, G., Yunes, J.A., da Silva, M.J., Vettore, A.L., Arruda, P., and Leite, A (1995). The involvement of Opaque 2 on beta-prolamin gene regulation in maize and Coix suggests a more general role for this transcriptional activator. *Plant molecular biology* 27, 1015-1029.

Pubmed: [Author and Title](#)

Google Scholar: [Author Only Title Only Author and Title](#)

de Vetten, N.C., and Ferl, R.J. (1995). Characterization of a maize G-box binding factor that is induced by hypoxia. *The Plant journal : for cell and molecular biology* 7, 589-601.

Pubmed: [Author and Title](#)

Google Scholar: [Author Only Title Only Author and Title](#)

Du, Z., Zhou, X., Ling, Y., Zhang, Z., and Su, Z. (2010). agriGO: a GO analysis toolkit for the agricultural community. *Nucleic acids research* 38, W64-70.

Pubmed: [Author and Title](#)

Google Scholar: [Author Only Title Only Author and Title](#)

Eveland, A.L., Goldshmidt, A., Pautler, M., Morohashi, K., Liseron-Monfils, C., Lewis, M.W., Kumari, S., Hiraga, S., Yang, F., Unger-Wallace, E., Olson, A., Hake, S., Vollbrecht, E., Grotewold, E., Ware, D., and Jackson, D. (2014). Regulatory modules controlling maize inflorescence architecture. *Genome research* 24, 431-443.

Pubmed: [Author and Title](#)

Google Scholar: [Author Only Title Only Author and Title](#)

FAO. (2015). FAO Statistical Pocketbook 2015. (<http://www.fao.org/documents/card/en/c/383d384a-28e6-47b3-a1a2-2496a9e017b2>).

Pubmed: [Author and Title](#)

Google Scholar: [Author Only Title Only Author and Title](#)

Feng, J., Liu, T., Qin, B., Zhang, Y., and Liu, X.S. (2012). Identifying ChIP-seq enrichment using MACS. *Nature protocols* 7, 1728-1740.

Pubmed: [Author and Title](#)

Google Scholar: [Author Only Title Only Author and Title](#)

Friedman, W.E., Madrid, E.N., and Williams, J.H. (2008). Origin of the fittest and survival of the fittest: Relating female gametophyte development to endosperm genetics. *Int J Plant Sci* 169, 79-92.

Pubmed: [Author and Title](#)

Google Scholar: [Author Only Title Only Author and Title](#)

Frizzi, A., Caldo, R.A., Morrell, J.A., Wang, M., Lutfiyya, L.L., Brown, W.E., Malvar, T.M., and Huang, S. (2010). Compositional and transcriptional analyses of reduced zein kernels derived from the opaque2 mutation and RNAi suppression. *Plant molecular biology* 73, 569-585.

Pubmed: [Author and Title](#)

Google Scholar: [Author Only Title Only Author and Title](#)

Gallusci, P., Varotto, S., Matsuko, M., Maddaloni, M., and Thompson, R.D. (1996). Regulation of cytosolic pyruvate, orthophosphate dikinase expression in developing maize endosperm. *Plant molecular biology* 31, 45-55.

Pubmed: [Author and Title](#)

Google Scholar: [Author Only Title Only Author and Title](#)

Gehl, C., Waadt, R., Kudla, J., Mendel, R.R., and Hansch, R. (2009). New GATEWAY vectors for high throughput analyses of protein-protein interactions by bimolecular fluorescence complementation. *Molecular plant* 2, 1051-1058.

Pubmed: [Author and Title](#)

Google Scholar: [Author Only Title Only Author and Title](#)

Gontarek, B.C., Neelakandan, A.K., Wu, H., and Becraft, P.W. (2016). NKD Transcription Factors Are Central Regulators of Maize Endosperm Development. *The Plant cell* 28, 2916-2936.

Pubmed: [Author and Title](#)

Google Scholar: [Author Only Title Only Author and Title](#)

Gotz, S., Garcia-Gomez, J.M., Terol, J., Williams, T.D., Nagaraj, S.H., Nueda, M.J., Robles, M., Talon, M., Dopazo, J., and Conesa, A. (2008). High-throughput functional annotation and data mining with the Blast2GO suite. *Nucleic acids research* 36, 3420-3435.

Pubmed: [Author and Title](#)

Google Scholar: [Author Only Title Only Author and Title](#)

Gray, J., Bevan, M., Brutnell, T., Buell, C.R., Cone, K., Hake, S., Jackson, D., Kellogg, E., Lawrence, C., McCouch, S., Mockler, T., Moose, S., Paterson, A., Peterson, T., Rokshar, D., Souza, G.M., Springer, N., Stein, N., Timmermans, M., Wang, G.L., and Grotewold, E. (2009). A recommendation for naming transcription factor proteins in the grasses. *Plant physiology* 149, 4-6.

Pubmed: [Author and Title](#)

Google Scholar: [Author Only Title Only Author and Title](#)

Hamamura, Y., Nagahara, S., and Higashiyama, T. (2012). Double fertilization on the move. *Current opinion in plant biology* 15, 70-77.

Pubmed: [Author and Title](#)

Google Scholar: [Author Only Title Only Author and Title](#)

Hartings, H., Lauria, M., Lazzaroni, N., Pirona, R., and Motto, M. (2011). The Zea mays mutants opaque-2 and opaque-7 disclose extensive changes in endosperm metabolism as revealed by protein, amino acid, and transcriptome-wide analyses. *BMC genomics* 12, 41.

Pubmed: [Author and Title](#)

Google Scholar: [Author Only Title Only Author and Title](#)

Hoecker, U., Vasil, I.K., and McCarty, D.R. (1995). Integrated control of seed maturation and germination programs by activator and

repressor functions of Viviparous-1 of maize. *Genes & development* 9, 2459-2469.

Pubmed: [Author and Title](#)

Google Scholar: [Author Only Title Only Author and Title](#)

Hoecker, U., Vasil, I.K., and McCarty, D.R. (1999). Signaling from the embryo conditions Vp1-mediated repression of alpha-amylase genes in the aleurone of developing maize seeds. *The Plant journal : for cell and molecular biology* 19, 371-377.

Pubmed: [Author and Title](#)

Google Scholar: [Author Only Title Only Author and Title](#)

Holding, D.R., Hunter, B.G., Chung, T., Gibbon, B.C., Ford, C.F., Bharti, A.K., Messing, J., Hamaker, B.R., and Larkins, B.A (2008). Genetic analysis of opaque2 modifier loci in quality protein maize. *TAG. Theoretical and applied genetics. Theoretische und angewandte Genetik* 117, 157-170.

Pubmed: [Author and Title](#)

Google Scholar: [Author Only Title Only Author and Title](#)

Hunter, B.G., Beatty, M.K., Singletary, G.W., Hamaker, B.R., Dilkes, B.P., Larkins, B.A, and Jung, R. (2002). Maize opaque endosperm mutations create extensive changes in patterns of gene expression. *The Plant cell* 14, 2591-2612.

Pubmed: [Author and Title](#)

Google Scholar: [Author Only Title Only Author and Title](#)

Hwang, Y.S., Ciceri, P., Parsons, R.L., Moose, S.P., Schmidt, R.J., and Huang, N. (2004). The maize O2 and PBF proteins act additively to promote transcription from storage protein gene promoters in rice endosperm cells. *Plant & cell physiology* 45, 1509-1518.

Pubmed: [Author and Title](#)

Google Scholar: [Author Only Title Only Author and Title](#)

Jia, H., Nettleton, D., Peterson, J.M., Vazquez-Carrillo, G., Jannink, J.L., and Scott, M.P. (2007). Comparison of transcript profiles in wild-type and o2 maize endosperm in different genetic backgrounds. *Crop Science* 47, S45-S59.

Pubmed: [Author and Title](#)

Google Scholar: [Author Only Title Only Author and Title](#)

Jia, M., Wu, H., Clay, K.L., Jung, R., Larkins, B.A, and Gibbon, B.C. (2013). Identification and characterization of lysine-rich proteins and starch biosynthesis genes in the opaque2 mutant by transcriptional and proteomic analysis. *BMC plant biology* 13, 60.

Pubmed: [Author and Title](#)

Google Scholar: [Author Only Title Only Author and Title](#)

Jin, J., Zhang, H., Kong, L., Gao, G., and Luo, J. (2014). PlantTFDB 3.0: a portal for the functional and evolutionary study of plant transcription factors. *Nucleic acids research* 42, D1182-1187.

Pubmed: [Author and Title](#)

Google Scholar: [Author Only Title Only Author and Title](#)

Kemper, E.L., Neto, G.C., Papes, F., Moraes, K.C., Leite, A., and Arruda, P. (1999). The role of opaque2 in the control of lysine-degrading activities in developing maize endosperm. *The Plant cell* 11, 1981-1994.

Pubmed: [Author and Title](#)

Google Scholar: [Author Only Title Only Author and Title](#)

Kent, W.J. (2002). BLAT--the BLAST-like alignment tool. *Genome research* 12, 656-664.

Pubmed: [Author and Title](#)

Google Scholar: [Author Only Title Only Author and Title](#)

Kodrzycki, R., Boston, R.S., and Larkins, B.A (1989). The opaque-2 mutation of maize differentially reduces zein gene transcription. *The Plant cell* 1, 105-114.

Pubmed: [Author and Title](#)

Google Scholar: [Author Only Title Only Author and Title](#)

Kusano, T., Berberich, T., Harada, M., Suzuki, N., and Sugawara, K. (1995). A maize DNA-binding factor with a bZIP motif is induced by low temperature. *Molecular & general genetics : MGG* 248, 507-517.

Pubmed: [Author and Title](#)

Google Scholar: [Author Only Title Only Author and Title](#)

Langmead, B., and Salzberg, S.L. (2012). Fast gapped-read alignment with Bowtie 2. *Nature methods* 9, 357-359.

Pubmed: [Author and Title](#)

Google Scholar: [Author Only Title Only Author and Title](#)

Larkins, B.A, Wu, Y., Song, R., and Messing, J. (2017). Maize Seed Storage Proteins. In *Maize Kernel Development*, B.A. Larkins, ed (CAB International), pp. 175-189.

Pubmed: [Author and Title](#)

Google Scholar: [Author Only Title Only Author and Title](#)

Leroux, B.M., Goodyke, A.J., Schumacher, K.I., Abbott, C.P., Clore, A.M., Yadegari, R., Larkins, B.A, and Dannenhoffer, J.M. (2014). Maize early endosperm growth and development: from fertilization through cell type differentiation. *American journal of botany* 101, 1259-1274.

Pubmed: [Author and Title](#)

Google Scholar: [Author Only Title Only Author and Title](#)

Li, C., Qiao, Z., Qi, W., Wang, Q., Yuan, Y., Yang, X., Tang, Y., Mei, B., Lv, Y., Zhao, H., Xiao, H., and Song, R. (2015). Genome-wide

characterization of cis-acting DNA targets reveals the transcriptional regulatory framework of opaque2 in maize. *The Plant cell* 27, 532-545.

Pubmed: [Author and Title](#)

Google Scholar: [Author Only Title Only Author and Title](#)

Li, G., Wang, D., Yang, R., Logan, K., Chen, H., Zhang, S., Skaggs, M.I., Lloyd, A., Burnett, W.J., Laurie, J.D., Hunter, B.G., Dannenhoffer, J.M., Larkins, B.A., Drews, G.N., Wang, X., and Yadegari, R. (2014). Temporal patterns of gene expression in developing maize endosperm identified through transcriptome sequencing. *Proceedings of the National Academy of Sciences of the United States of America* 111, 7582-7587.

Pubmed: [Author and Title](#)

Google Scholar: [Author Only Title Only Author and Title](#)

Li, J., and Berger, F. (2012). Endosperm: food for humankind and fodder for scientific discoveries. *The New phytologist* 195, 290-305.

Pubmed: [Author and Title](#)

Google Scholar: [Author Only Title Only Author and Title](#)

Li, Q., Wang, J., Ye, J., Zheng, X., Xiang, X., Li, C., Fu, M., Wang, Q., Zhang, Z.Y., and Wu, Y. (2017). The Maize Imprinted Gene *Floury3* Encodes a PLATZ Protein Required for tRNA and 5S rRNA Transcription Through Interaction with RNA Polymerase III. *The Plant cell*.

Pubmed: [Author and Title](#)

Google Scholar: [Author Only Title Only Author and Title](#)

Locatelli, S., Piatti, P., Motto, M., and Rossi, V. (2009). Chromatin and DNA modifications in the Opaque2-mediated regulation of gene transcription during maize endosperm development. *The Plant cell* 21, 1410-1427.

Pubmed: [Author and Title](#)

Google Scholar: [Author Only Title Only Author and Title](#)

Lohmer, S., Maddaloni, M., Motto, M., Di Fonzo, N., Hartings, H., Salamini, F., and Thompson, R.D. (1991). The maize regulatory locus Opaque-2 encodes a DNA-binding protein which activates the transcription of the b-32 gene. *The EMBO journal* 10, 617-624.

Pubmed: [Author and Title](#)

Google Scholar: [Author Only Title Only Author and Title](#)

Machanick, P., and Bailey, T.L. (2011). MEME-ChIP: motif analysis of large DNA datasets. *Bioinformatics* 27, 1696-1697.

Pubmed: [Author and Title](#)

Google Scholar: [Author Only Title Only Author and Title](#)

Maddaloni, M., Di Fonzo, N., Hartings, H., Lazzaroni, N., Salamini, F., Thompson, R., and Motto, M. (1989). The sequence of the zein regulatory gene opaque-2 (O2) of Zea Mays. *Nucleic acids research* 17, 7532.

Pubmed: [Author and Title](#)

Google Scholar: [Author Only Title Only Author and Title](#)

Maddaloni, M., Donini, G., Balconi, C., Rizzi, E., Gallusci, P., Forlani, F., Lohmer, S., Thompson, R., Salamini, F., and Motto, M. (1996). The transcriptional activator Opaque-2 controls the expression of a cytosolic form of pyruvate orthophosphate dikinase-1 in maize endosperms. *Molecular & general genetics : MGG* 250, 647-654.

Pubmed: [Author and Title](#)

Google Scholar: [Author Only Title Only Author and Title](#)

Mangan, S., and Alon, U. (2003). Structure and function of the feed-forward loop network motif. *Proceedings of the National Academy of Sciences of the United States of America* 100, 11980-11985.

Pubmed: [Author and Title](#)

Google Scholar: [Author Only Title Only Author and Title](#)

Mathelier, A., Zhao, X., Zhang, A.W., Parcy, F., Worsley-Hunt, R., Arenillas, D.J., Buchman, S., Chen, C.Y., Chou, A., Ienasescu, H., Lim, J., Shyr, C., Tan, G., Zhou, M., Lenhard, B., Sandelin, A., and Wasserman, W.W. (2014). JASPAR 2014: an extensively expanded and updated open-access database of transcription factor binding profiles. *Nucleic acids research* 42, D142-147.

Pubmed: [Author and Title](#)

Google Scholar: [Author Only Title Only Author and Title](#)

Mertz, E.T., Bates, L.S., and Nelson, O.E. (1964). Mutant gene that changes protein composition and increases lysine content of maize endosperm. *Science* 145, 279-280.

Pubmed: [Author and Title](#)

Google Scholar: [Author Only Title Only Author and Title](#)

Morohashi, K., Casas, M.I., Falcone Ferreyra, M.L., Mejia-Guerra, M.K., Pourcel, L., Yilmaz, A., Feller, A., Carvalho, B., Emiliani, J., Rodriguez, E., Pellegrinet, S., McMullen, M., Casati, P., and Grotewold, E. (2012). A genome-wide regulatory framework identifies maize pericarp color1 controlled genes. *The Plant cell* 24, 2745-2764.

Pubmed: [Author and Title](#)

Google Scholar: [Author Only Title Only Author and Title](#)

Muth, J.R., Muller, M., Lohmer, S., Salamini, F., and Thompson, R.D. (1996). The role of multiple binding sites in the activation of zein gene expression by Opaque-2. *Molecular & general genetics : MGG* 252, 723-732.

Pubmed: [Author and Title](#)

Google Scholar: [Author Only Title Only Author and Title](#)

Olsen, O.A (2001). ENDOSPERM DEVELOPMENT: Cellularization and Cell Fate Specification. *Annual review of plant physiology and*

plant molecular biology 52, 233-267.

Pubmed: [Author and Title](#)

Google Scholar: [Author Only Title Only Author and Title](#)

Olsen, O.A (2004). Nuclear endosperm development in cereals and *Arabidopsis thaliana*. *The Plant cell* 16 Suppl, S214-227.

Pubmed: [Author and Title](#)

Google Scholar: [Author Only Title Only Author and Title](#)

Pysh, L.D., and Schmidt, R.J. (1996). Characterization of the maize OHP1 gene: evidence of gene copy variability among inbreds. *Gene* 177, 203-208.

Pubmed: [Author and Title](#)

Google Scholar: [Author Only Title Only Author and Title](#)

Pysh, L.D., Aukerman, M.J., and Schmidt, R.J. (1993). OHP1: a maize basic domain/leucine zipper protein that interacts with opaque2. *The Plant cell* 5, 227-236.

Pubmed: [Author and Title](#)

Google Scholar: [Author Only Title Only Author and Title](#)

Qiao, Z, Qi, W., Wang, Q., Feng, Y., Yang, Q., Zhang, N., Wang, S., Tang, Y., and Song, R. (2016). ZmMADS47 Regulates Zein Gene Transcription through Interaction with Opaque2. *PLoS genetics* 12, e1005991.

Pubmed: [Author and Title](#)

Google Scholar: [Author Only Title Only Author and Title](#)

Quinlan, A.R., and Hall, I.M. (2010). BEDTools: a flexible suite of utilities for comparing genomic features. *Bioinformatics* 26, 841-842.

Pubmed: [Author and Title](#)

Google Scholar: [Author Only Title Only Author and Title](#)

Robinson, M.D., McCarthy, D.J., and Smyth, G.K. (2010). edgeR: a Bioconductor package for differential expression analysis of digital gene expression data. *Bioinformatics* 26, 139-140.

Pubmed: [Author and Title](#)

Google Scholar: [Author Only Title Only Author and Title](#)

Sabelli, P.A., and Larkins, B.A (2009). The development of endosperm in grasses. *Plant physiology* 149, 14-26.

Pubmed: [Author and Title](#)

Google Scholar: [Author Only Title Only Author and Title](#)

Saleh, A, Alvarez-Venegas, R., and Avramova, Z. (2008). An efficient chromatin immunoprecipitation (ChIP) protocol for studying histone modifications in *Arabidopsis* plants. *Nature protocols* 3, 1018-1025.

Pubmed: [Author and Title](#)

Google Scholar: [Author Only Title Only Author and Title](#)

Schmidt, R.J., Burr, F.A., and Burr, B. (1987). Transposon tagging and molecular analysis of the maize regulatory locus opaque-2. *Science* 238, 960-963.

Pubmed: [Author and Title](#)

Google Scholar: [Author Only Title Only Author and Title](#)

Schmidt, R.J., Burr, F.A., Aukerman, M.J., and Burr, B. (1990). Maize regulatory gene opaque-2 encodes a protein with a "leucine-zipper" motif that binds to zein DNA. *Proceedings of the National Academy of Sciences of the United States of America* 87, 46-50.

Pubmed: [Author and Title](#)

Google Scholar: [Author Only Title Only Author and Title](#)

Schmidt, R.J., Ketudat, M., Aukerman, M.J., and Hoschek, G. (1992). Opaque-2 is a transcriptional activator that recognizes a specific target site in 22-kD zein genes. *The Plant cell* 4, 689-700.

Pubmed: [Author and Title](#)

Google Scholar: [Author Only Title Only Author and Title](#)

Sievers, F., Wilm, A., Dineen, D., Gibson, T.J., Karplus, K., Li, W.Z., Lopez, R., McWilliam, H., Remmert, M., Soding, J., Thompson, J.D., and Higgins, D.G. (2011). Fast, scalable generation of high-quality protein multiple sequence alignments using Clustal Omega. *Mol Syst Biol* 7.

Pubmed: [Author and Title](#)

Google Scholar: [Author Only Title Only Author and Title](#)

Stamatakis, A (2014). RAxML version 8: a tool for phylogenetic analysis and post-analysis of large phylogenies. *Bioinformatics* 30, 1312-1313.

Pubmed: [Author and Title](#)

Google Scholar: [Author Only Title Only Author and Title](#)

Taylor-Teeple, M., Lin, L., de Lucas, M., Turco, G., Toal, T.W., Gaudinier, A., Young, N.F., Trabucco, G.M., Veling, M.T., Lamothe, R., Handakumbura, P.P., Xiong, G., Wang, C., Corwin, J., Tsoukalas, A., Zhang, L., Ware, D., Pauly, M., Kliebenstein, D.J., Dehesh, K., Tagkopoulos, I., Breton, G., Pruneda-Paz, J.L., Ahnert, S.E., Kay, S.A., Hazen, S.P., and Brady, S.M. (2015). An *Arabidopsis* gene regulatory network for secondary cell wall synthesis. *Nature* 517, 571-575.

Pubmed: [Author and Title](#)

Google Scholar: [Author Only Title Only Author and Title](#)

Thorvaldsdottir, H., Robinson, J.T., and Mesirov, J.P. (2013). Integrative Genomics Viewer (IGV): high-performance genomics data

visualization and exploration. *Briefings in bioinformatics* 14, 178-192.

Pubmed: [Author and Title](#)

Google Scholar: [Author Only Title Only Author and Title](#)

Trapnell, C., Pachter, L., and Salzberg, S.L. (2009). TopHat: discovering splice junctions with RNA-Seq. *Bioinformatics* 25, 1105-1111.

Pubmed: [Author and Title](#)

Google Scholar: [Author Only Title Only Author and Title](#)

Unger, E., Parsons, R.L., Schmidt, R.J., Bowen, B., and Roth, B.A (1993). Dominant Negative Mutants of Opaque2 Suppress Transactivation of a 22-kD Zein Promoter by Opaque2 in Maize Endosperm Cells. *The Plant cell* 5, 831-841.

Pubmed: [Author and Title](#)

Google Scholar: [Author Only Title Only Author and Title](#)

Vicente-Carabajosa, J., Moose, S.P., Parsons, R.L., and Schmidt, R.J. (1997). A maize zinc-finger protein binds the prolamin box in zein gene promoters and interacts with the basic leucine zipper transcriptional activator Opaque2. *Proceedings of the National Academy of Sciences of the United States of America* 94, 7685-7690.

Pubmed: [Author and Title](#)

Google Scholar: [Author Only Title Only Author and Title](#)

Walley, J.W., Shen, Z., Sartor, R., Wu, K.J., Osborn, J., Smith, L.G., and Briggs, S.P. (2013). Reconstruction of protein networks from an atlas of maize seed proteotypes. *Proceedings of the National Academy of Sciences of the United States of America* 110, E4808-4817.

Pubmed: [Author and Title](#)

Google Scholar: [Author Only Title Only Author and Title](#)

Walsh, J.R., Schaeffer, M.L., Zhang, P., Rhee, S.Y., Dickerson, J.A., and Sen, T.Z (2016). The quality of metabolic pathway resources depends on initial enzymatic function assignments: a case for maize. *BMC systems biology* 10, 129.

Pubmed: [Author and Title](#)

Google Scholar: [Author Only Title Only Author and Title](#)

Wang, D., Tyson, M.D., Jackson, S.S., and Yadegari, R. (2006). Partially redundant functions of two SET-domain polycomb-group proteins in controlling initiation of seed development in *Arabidopsis*. *Proceedings of the National Academy of Sciences of the United States of America* 103, 13244-13249.

Pubmed: [Author and Title](#)

Google Scholar: [Author Only Title Only Author and Title](#)

Wang, D., Zhang, C., Hearn, D.J., Kang, I.H., Punwani, J.A., Skaggs, M.I., Drews, G.N., Schumaker, K.S., and Yadegari, R. (2010). Identification of transcription-factor genes expressed in the *Arabidopsis* female gametophyte. *BMC plant biology* 10, 110.

Pubmed: [Author and Title](#)

Google Scholar: [Author Only Title Only Author and Title](#)

Whelan, S., and Goldman, N. (2001). A general empirical model of protein evolution derived from multiple protein families using a maximum-likelihood approach. *Molecular biology and evolution* 18, 691-699.

Pubmed: [Author and Title](#)

Google Scholar: [Author Only Title Only Author and Title](#)

Woo, Y.M., Hu, D.W., Larkins, B.A., and Jung, R. (2001). Genomics analysis of genes expressed in maize endosperm identifies novel seed proteins and clarifies patterns of zein gene expression. *The Plant cell* 13, 2297-2317.

Pubmed: [Author and Title](#)

Google Scholar: [Author Only Title Only Author and Title](#)

Wu, Y., and Messing, J. (2012). Rapid divergence of prolamin gene promoters of maize after gene amplification and dispersal. *Genetics* 192, 507-519.

Pubmed: [Author and Title](#)

Google Scholar: [Author Only Title Only Author and Title](#)

Wu, Y., and Messing, J. (2014). Proteome balancing of the maize seed for higher nutritional value. *Frontiers in plant science* 5, 240.

Pubmed: [Author and Title](#)

Google Scholar: [Author Only Title Only Author and Title](#)

Xu, J.H., and Messing, J. (2008). Diverged copies of the seed regulatory Opaque-2 gene by a segmental duplication in the progenitor genome of rice, sorghum, and maize. *Molecular plant* 1, 760-769.

Pubmed: [Author and Title](#)

Google Scholar: [Author Only Title Only Author and Title](#)

Yan, D., Duermeyer, L., Leoveanu, C., and Nambara, E. (2014). The Functions of the Endosperm During Seed Germination. *Plant & cell physiology* 55, 1521-1533.

Pubmed: [Author and Title](#)

Google Scholar: [Author Only Title Only Author and Title](#)

Yang, J., Ji, C., and Wu, Y. (2016). Divergent Transactivation of Maize Storage Protein Zein Genes by the Transcription Factors Opaque2 and OHPs. *Genetics* 204, 581-591.

Pubmed: [Author and Title](#)

Google Scholar: [Author Only Title Only Author and Title](#)

Yi, G., Neelakandan, A.K., Gontarek, B.C., Vollbrecht, E., and Becroft, P.W. (2015). The naked endosperm genes encode duplicate

INDETERMINATE domain transcription factors required for maize endosperm cell patterning and differentiation. Plant physiology 167, 443-456.

Pubmed: [Author and Title](#)

Google Scholar: [Author Only Title Only Author and Title](#)

Yilmaz, A., Nishiyama, M.Y., Jr., Fuentes, B.G., Souza, G.M., Janies, D., Gray, J., and Grotewold, E. (2009). GRASSIUS: a platform for comparative regulatory genomics across the grasses. Plant physiology 149, 171-180.

Pubmed: [Author and Title](#)

Google Scholar: [Author Only Title Only Author and Title](#)

Zhan, J., Dannenhoffer, J.M., and Yadegari, R. (2017). Endosperm Development and Cell Specialization. In Maize Kernel Development, B.A Larkins, ed (CAB International), pp. 28-43.

Pubmed: [Author and Title](#)

Google Scholar: [Author Only Title Only Author and Title](#)

Zhan, J., Thakare, D., Ma, C., Lloyd, A., Nixon, N.M., Arakaki, A.M., Burnett, W.J., Logan, K.O., Wang, D., Wang, X., Drews, G.N., and Yadegari, R. (2015). RNA sequencing of laser-capture microdissected compartments of the maize kernel identifies regulatory modules associated with endosperm cell differentiation. The Plant cell 27, 513-531.

Pubmed: [Author and Title](#)

Google Scholar: [Author Only Title Only Author and Title](#)

Zhang, Y., Liu, T., Meyer, C.A., Eeckhoute, J., Johnson, D.S., Bernstein, B.E., Nusbaum, C., Myers, R.M., Brown, M., Li, W., and Liu, X.S. (2008). Model-based analysis of ChIP-Seq (MACS). Genome biology 9, R137.

Pubmed: [Author and Title](#)

Google Scholar: [Author Only Title Only Author and Title](#)

Zhang, Z., Yang, J., and Wu, Y. (2015). Transcriptional Regulation of Zein Gene Expression in Maize through the Additive and Synergistic Action of opaque2, Prolamine-Box Binding Factor, and O2 Heterodimerizing Proteins. The Plant cell 27, 1162-1172.

Pubmed: [Author and Title](#)

Google Scholar: [Author Only Title Only Author and Title](#)

Zhang, Z., Zheng, X., Yang, J., Messing, J., and Wu, Y. (2016). Maize endosperm-specific transcription factors O2 and PBF network the regulation of protein and starch synthesis. Proceedings of the National Academy of Sciences of the United States of America 113, 10842-10847.

Pubmed: [Author and Title](#)

Google Scholar: [Author Only Title Only Author and Title](#)

Opaque-2 Regulates a Complex Gene Network Associated with Cell Differentiation and Storage Functions of Maize Endosperm

Junpeng Zhan, Guosheng Li, Choong-Hwan Ryu, Chuang Ma, Shanshan Zhang, Alan Lloyd, Brenda G. Hunter, Brian A. Larkins, Gary N. Drews, Xiangfeng Wang and Ramin Yadegari
Plant Cell; originally published online September 27, 2018;
DOI 10.1105/tpc.18.00392

This information is current as of October 30, 2018

Supplemental Data	/content/suppl/2018/10/14/tpc.18.00392.DC2.html /content/suppl/2018/09/27/tpc.18.00392.DC1.html
Permissions	https://www.copyright.com/ccc/openurl.do?sid=pd_hw1532298X&issn=1532298X&WT.mc_id=pd_hw1532298X
eTOCs	Sign up for eTOCs at: http://www.plantcell.org/cgi/alerts/ctmain
CiteTrack Alerts	Sign up for CiteTrack Alerts at: http://www.plantcell.org/cgi/alerts/ctmain
Subscription Information	Subscription Information for <i>The Plant Cell</i> and <i>Plant Physiology</i> is available at: http://www.aspб.org/publications/subscriptions.cfm